iScience

CellPress
OPEN ACCESS

Article

Radiotolerance of N-cycle bacteria and their transcriptomic response to low-dose space-analogue ionizing irradiation

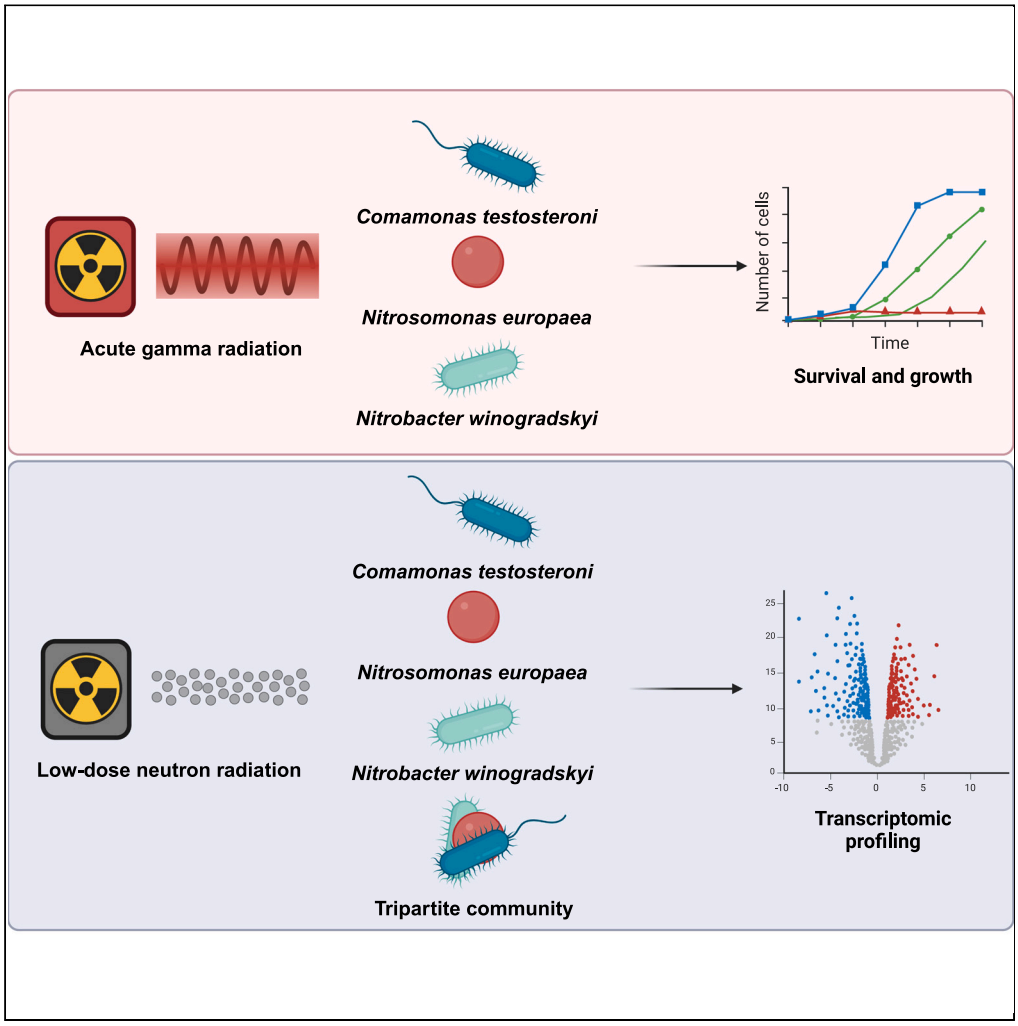

Tom Verbeelen, Celia Alvarez Fernandez, Thanh Huy Nguyen, ..., Natalie Leys, Ramon Ganigué, Felice Mastroleo

felice.mastroleo@sckcen.be

Highlights

C. testosteroni, *N. europaea*, and *N. winogradskyi* are radiosensitive strains

D_{10}-value of *C. testosteroni* I2 was determined at 87.99 ± 1.21 Gy

Whole transcriptome analysis after exposure to low-dose ionizing radiation

Low-dose ionizing radiation has limited impact on nitrification related genes

Verbeelen et al., iScience *27*, 109596
May 17, 2024
https://doi.org/10.1016/j.isci.2024.109596

iScience

CellPress
OPEN ACCESS

Article

Radiotolerance of N-cycle bacteria and their transcriptomic response to low-dose space-analogue ionizing irradiation

Tom Verbeelen,[1,2] Celia Alvarez Fernandez,[2] Thanh Huy Nguyen,[3] Surya Gupta,[1] Baptiste Leroy,[3] Ruddy Wattiez,[3] Siegfried E. Vlaeminck,[4,5] Natalie Leys,[1] Ramon Ganigué,[2,5] and Felice Mastroleo[1,6,*]

SUMMARY

The advancement of regenerative life support systems (RLSS) is crucial to allow long-distance space travel. Within the Micro-Ecological Life Support System Alternative (MELiSSA), efficient nitrogen recovery from urine and other waste streams is vital to produce liquid fertilizer to feed food and oxygen production in subsequent photoautotrophic processes. This study explores the effects of ionizing radiation on nitrogen cycle bacteria that transform urea to nitrate. In particular, we assess the radiotolerance of *Comamonas testosteroni*, *Nitrosomonas europaea*, and *Nitrobacter winogradskyi* after exposure to acute γ-irradiation. Moreover, a comprehensive whole transcriptome analysis elucidates the effects of spaceflight-analogue low-dose ionizing radiation on the individual axenic strains and on their synthetic community o. This research sheds light on how the spaceflight environment could affect ureolysis and nitrification processes from a transcriptomic perspective.

INTRODUCTION

By harnessing biological processes, regenerative life support systems (RLSS) offer a sustainable solution to recycle and regenerate essential resources in isolated environments. The systems represent state-of-the-art technology with great promise for enabling long-distance space travel. In space exploration, RLSSs create a self-sustaining environment that minimizes reliance on resupply flights from Earth. The European Space Agency (ESA)'s Micro-Ecological Life Support Alternative (MELiSSA) program is an advanced RLSS project composed of 5 interconnected compartments.[1,2] Each compartment is populated by one or more (micro)organisms serving a specific purpose. Compartment III (CIII) currently enables the recovery of nitrogen from NH_4^+ by converting it to NO_3^-. NO_3^-, in turn, serves as a nitrogen source for higher plants and cyanobacteria in compartment IV for food and O_2 production.[1] It is currently occupied by a synthetic bacterial community of nitrification bacteria, i.e., *Nitrosomonas europaea* and *Nitrobacter winogradskyi*. This configuration is unable to directly treat urine due to the nitrifiers' inability to convert urea. Urine holds 85% of recoverable nitrogen in an RLSS as urea. For this reason, a third constituent should be added to the consortium that is capable of hydrolyzing urea to NH_4^+ in a process called ureolysis, expanding the original CIII with the additional functionality of urine treatment. The feasibility of adding the heterotrophic, gram-negative ureolytic *Comamonas testosteroni* to the nitrifying culture has already been demonstrated.[3] In the context of an RLSS for spaceflight applications, the consortium's viability during spaceflight and the effects of the spaceflight environment on the bacteria have to be properly characterized.

Environmental conditions in space are very hostile to human and bacterial survival. These factors include a state of altered gravity and enhanced ionizing radiation (IR) dose rates. In low-Earth orbit (LEO), IR dose rates can range from 400 to 630 μGy d^{-1}[4–6] while inside the International Space Station (ISS) located in LEO, the average dose rate is 280 μGy d^{-1}.[7] LEO and Earth are protected by the Earth's magnetosphere, reducing the impact of galactic cosmic rays 10-fold.[8] Beyond LEO, IR dose rates increase significantly and will be a major factor to consider during long-distance space travel. IR causes direct DNA damage by inducing single-strand and double-strands breaks (DSB).[9,10] In addition, IR generates reactive oxygen species (ROS) by interacting with H_2O molecules.[11–14] ROS like O_2^- (superoxide) and H_2O_2 cannot damage DNA directly. However, H_2O_2 can react with free intracellular Fe^{2+} through the Fenton reaction, generating Fe^{3+} and the highly reactive OH· radical. This radical is short-lived, but can cause damage to biomolecules. Specifically, Fe^{2+} ions associated with DNA can cause harmful mutagenic effects when reacting with ROS. Moreover, O_2^- facilitates the reduction of Fe^{3+} to Fe^{2+}, thereby maintaining the available

[1]Nuclear Medical Applications (NMA), Belgian Nuclear Research Centre (SCK CEN), Boeretang 200, 2400 Mol, Belgium
[2]Center for Microbial Ecology and Technology (CMET), Ghent University, Coupure Links 653, 9000 Ghent, Belgium
[3]Department of Proteomics and Microbiology, University of Mons, Av. Du Champs de Mars 6, 7000 Mons, Belgium
[4]Research Group of Sustainable Energy, Air and Water Technology, Department of Bioscience Engineering, University of Antwerp, Groenenborgerlaan 171, 2020 Antwerp, Belgium
[5]Centre for Advanced Process Technology for Urban REsource Recovery (CAPTURE), Frieda Saeysstraat 1, 9052 Ghent, Belgium
[6]Lead contact
*Correspondence: felice.mastroleo@sckcen.be
https://doi.org/10.1016/j.isci.2024.109596

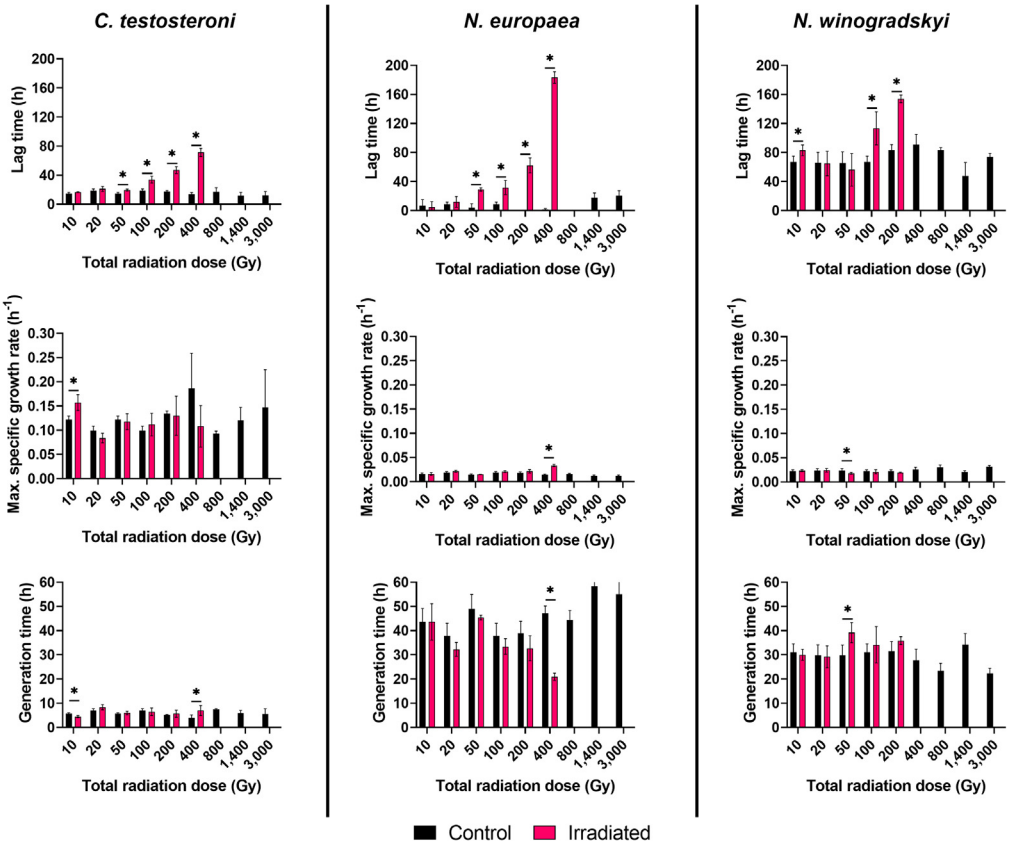

Figure 1. Growth kinetic parameters of *Comamonas testosteroni, Nitrosomonas europaea* and *Nitrobacter winogradskyi* after exposure to acute γ-radiation

Data is represented as mean ± SD (n = 4). Unpaired t-tests were performed between the control and the irradiated samples to identify significant differences: *$p < 0.05$.

Fe^{2+}-pool for the Fenton reaction.[15] As a result, IR is known to induce the oxidative stress response, DNA repair mechanisms, changes to the cell envelope, and can significantly affect growth rate in bacteria.[9,14,16]

In this study, we intended to monitor the tolerance and response of CIII-populating bacteria *C. testosteroni*, *N. europaea*, and *N. winogradskyi* to space-like IR, in the frame of the forthcoming Urine Nitrification in Space (URINIS) experiment. To achieve this, these strains were subjected to low-dose ISS-like IR. Their transcriptomic response was characterized individually in axenic cultures and together in a tripartite community setting, and the effect on ureolysis and nitrification genes was assessed. In the tripartite culture, relative cell densities were assessed to identify how low-dose ISS-like IR affects growth conditions for one strain compared to the other strains in the tripartite community. Moreover, radiotolerance of the axenic cultures was determined by exposing them to high-dose γ-radiation. This study provides valuable insights on the impact of low-dose IR on gene expression and an indication of radiotolerance of the N-cycle bacteria.

RESULTS

Effects of acute IR on growth kinetics and viability of N-cycle bacteria

Growth curves of axenic cultures after exposure to acute γ-radiation and subsequent inoculation in fresh SUSS medium are provided in Figures S1–S3. *C. testosteroni* and *N. europaea* did not proliferate after exposure to a total absorbed dose (D_T) of 800 Gy or higher, while no growth was observed from 400 Gy and higher for *N. winogradskyi*. Acute IR seemed to affect the lag time (λ) of all bacterial cultures (Figure 1). For *C. testosteroni*, the lag time increased from 16.68 ± 0.58 h after 10 Gy to 71.23 ± 5.67 h after 400 Gy of exposure. *N. europaea* required 4.66 ± 7.52 h to enter the exponential phase after 10 Gy and needed 183.25 ± 8.00 h after 400 Gy. Finally, the lag time of *N. winogradskyi* increased from 83.01 ± 7.38 h to 153.81 ± 5.25 h from 10 Gy to 200 Gy of exposure. The parameter increased with higher radiation exposure up until no growth was observed. For generation time (T) and max. specific growth rate (μ_{max}), significant differences ($p < 0.05$) were observed for several doses. However, no pattern was observed for different irradiation doses for these parameters.

Activity tests (Figures S4 and S5) confirmed the results of the growth curves for *N. europaea*. NH_4^+ consumption and NO_2^- production were reported for samples that were irradiated with 10, 20, 50, 100 and 200 Gy, but the onset of nitritation was delayed with increasing

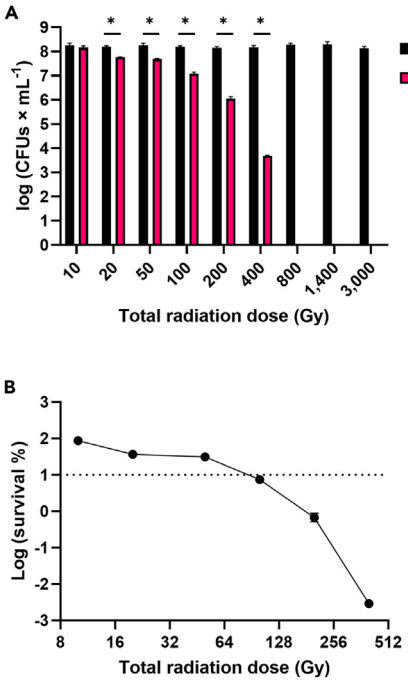

Figure 2. Survival of *Comamonas testosteroni* after acute γ-irradiation

(A) Log of colony-forming units (CFUs) per mL of *C. testosteroni* after exposure to acute gamma radiation.

(B) Log of the survival percentage of bacteria after exposure to acute γ-radiation. The dotted line represents 10% survival and D_{10} is situated at the intersection between the data and this threshold. Data is represented as mean ± SD (n = 4). Unpaired t-tests were performed between the control and the irradiated samples to identify significant differences: *$p < 0.05$.

irradiation in *N. europaea*. From 400 Gy and higher radiation doses, no activity was observed during the 10+ days of monitoring time. The same is true for NO_2^- consumption by *N. winogradskyi* (Figure S6).

Colony-forming unit (CFU) counting in *C. testosteroni* enabled a more accurate determination of its viability after radiation exposure. The number of CFUs decreased strongly with increasing irradiation ($p < 0.05$) vs. the non-irradiated cultures (Figure 2A). From these results, a survival curve was plotted based on the percentage of CFUs × mL^{-1} of irradiated samples vs. the control samples (Figure 2B). 87.99 ± 1.21 Gy was determined as the D_{10}-value (decimal reduction dose), representing the amount of radiation required to cause a 90% reduction in bacterial viability.

Construction of a survival curve for *N. europaea* and *N. winogradskyi* was attempted by determining the amount of energetically active cells (EAC) per mL after irradiation, since these autotrophic bacteria do not form colonies on LB agar plates. However, the used kit seemed to be inadequate to lyse *N. winogradskyi* cells because detected EAC × mL^{-1} values were close to the blank value. *N. europaea* displayed decreasing viability with increasing D_T ($p < 0.05$) but did not decrease below 10% of control values at 800 Gy and 1,400 Gy (Figure S7).

Effect of low-dose ISS-like IR exposure on growth of N-cycle bacteria

OD_{600} measurements of axenic *C. testosteroni* cultures after exposure to low-dose ISS-like IR were significantly higher ($p < 0.05$) than those of non-irradiated control cultures (Figure 3A). Cell densities of axenic cultures of the nitrifiers and the tripartite culture did not differ from their controls. Also, a quantitative PCR (qPCR) analysis was performed on DNA extracted from the tripartite culture to quantify the relative abundancy of each strain within the synthetic community (Figure 3B). In the control cultures and the irradiated cultures, *C. testosteroni* respectively made up 97.07% and 97.24% of the tripartite culture. *N. europaea* and *N. winogradskyi* respectively contributed 2.42% and 2.23% and 0.51% and 0.52% of the community. The relative abundance of the nitrifiers relative to each other was 82.47% and 17.53%, and 81.00% and 19.00% for *N. europaea* and *N. winogradskyi* in non-irradiated and irradiated samples, respectively. No significant differences were observed in the relative abundances of irradiated and control samples.

Comparative transcriptome analysis of N-cycle bacteria in axenic and tripartite culture after exposure to low-dose IR

Whole transcriptome analysis was performed on the axenic cultures and tripartite community after exposure to low-dose IR (Figure 6). Genes with a $|\log_2 FC| \leq 1$ ($|FC| \geq 2$) and a *p* value <0.05 were considered differentially expressed. An overview of all differentially expressed genes (DEGs) per strain is provided in the Data S1. An overview of the number of identified DEGs per strains is provided in Table 1. In the tripartite culture, a significant percentage of the total protein coding sequences (CDS) of the genomes of *C. testosteroni* (42.61%) and *N. winogradskyi* (61.14%) were not detected because only a limited portion of the mRNA reads could be mapped to their genomes. Nonetheless, differential gene expression (DGE) analysis was still performed to assess the effect of IR on the gene expression of these strains in a tripartite culture.

DEGs were annotated to different clusters of orthologous genes (COG)s. The number of overlapping DEGs of the strains in axenic vs. the tripartite culture are displayed in a Venn diagram (Figure 4). For the COGs, the percentage of DEGs annotated to that specific COG compared to the total number of DEGs was calculated. For *C. testosteroni*, 17.81% and 11.11% of all DEGs could not be attributed to a specific COG for

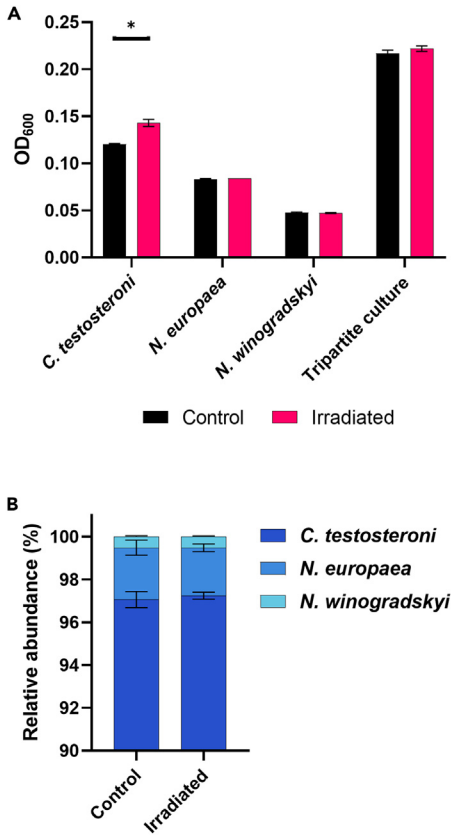

Figure 3. Effect of low-dose ISS-like ionizing radiation exposure on growth and relative abundance of N-cycle bacteria

(A) Endpoint OD_{600} measurements of the tripartite culture and (B) relative abundance of the three constituents of the tripartite community. Data is represented as mean ± SD (n = 4). Unpaired t-tests were performed between the control and the irradiated samples to identify significant differences: *$p < 0.05$.

the axenic and tripartite culture, respectively. We observed that three COGs out of the top five most affected COGs were recurrent in both cultures. These COGs were 'Amino acid transport and metabolism' (5.26% and 11.11%), 'Transcription' (6.88% and 5.98%) and 'Inorganic ion transport and metabolism' (5.26% and 5.98%). Eight overlapping DEGs were identified, coding for a putative 5-dehydro-4-deoxyglucarate dehydratase (JMRS01_350007), NADH-ubiquinone oxidoreductase subunit 6 (JMRS01_380058), an AAA domain-containing protein (JMRS01_420017), 50S ribosomal protein L25 (JMRS01_700035), an uncharacterized peroxidase-related enzyme (JMRS01_810045), a hypothetical protein (JMRS01_860090), D-3-phosphoglycerate dehydrogenase (JMRS01_910018) and 50S ribosomal protein L28 (JMRS01_1050094).

IR had a very limited effect on the transcriptomic profiles of both axenic and tripartite *N. europaea*. COG analysis (Figure 4B) revealed that 'Inorganic ion transport and metabolism' (Axenic: 14.08%, Tripartite: 8.70%) and 'Transcription' (Axenic: 12.68%, Tripartite: 4.35%) overlapped

Table 1. Overview of the number of DEGs (|FC| ≥ 2, *p* value <0.05) detected in axenic cultures and in the tripartite community of *Comamonas testosteroni*, *Nitrosomonas europaea* and *Nitrobacter winogradskyi*

Strain	Total CDS in genome	Detected CDS	DEGs	% of detected CDS	Upregulated DEGs	Downregulated DEGs
Axenic cultures						
C. testosteroni	5771	5763	247	4.29	139	108
N. europaea	2783	2710	71	2.62	17	54
N. winogradskyi	3649	3309	44	1.33	14	30
Tripartite culture						
C. testosteroni	5771	3312	117	3.53	81	36
N. europaea	2783	2710	23	0.89	6	17
N. winogradskyi	3649	1418	102	7.19	19	83

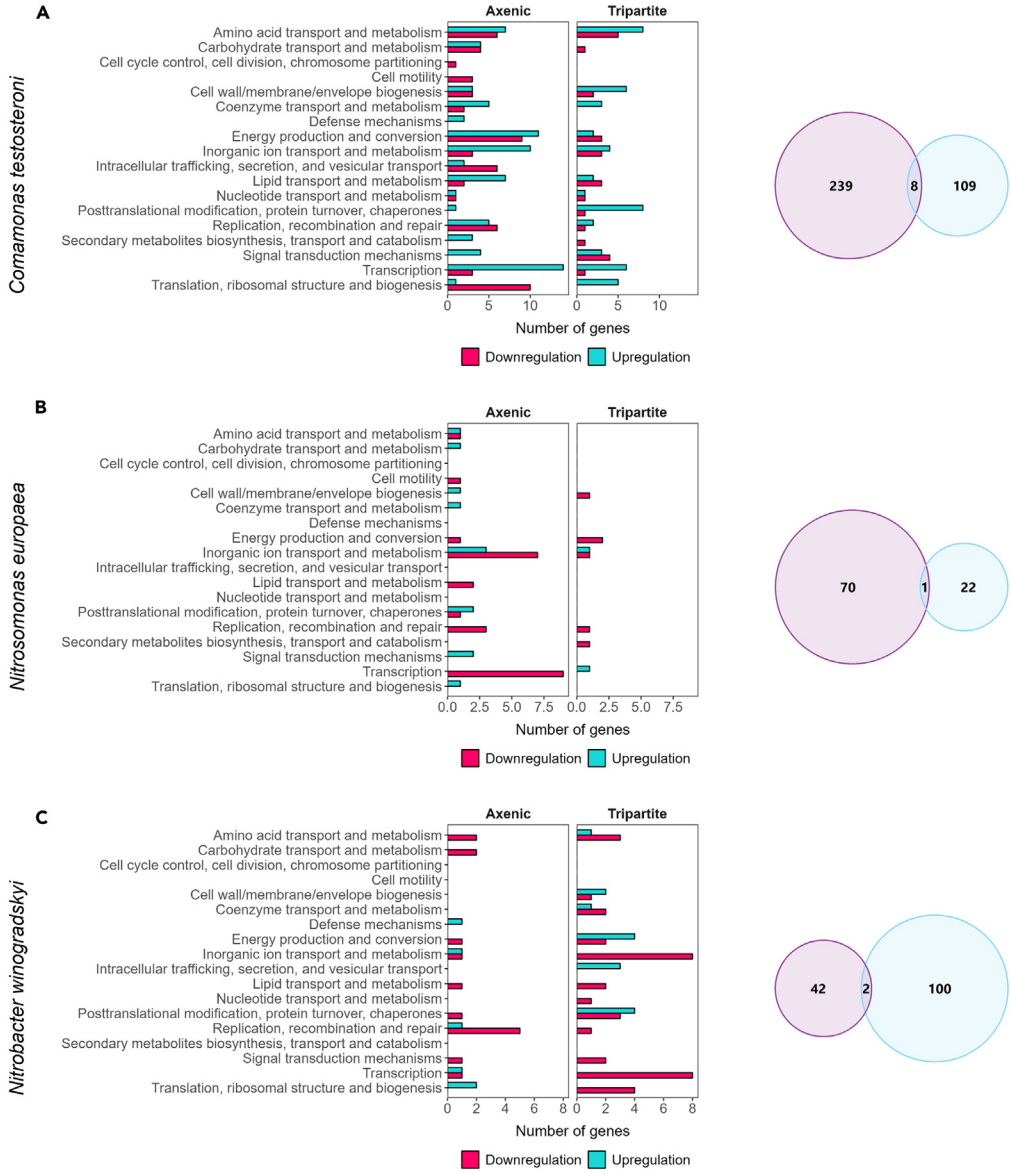

Figure 4. Comparative transcriptomic analysis of N-cycle bacteria in axenic and tripartite culture after exposure to low-dose ionizing radiation

COG analysis and Venn diagrams of overlapping DEGs for axenic (purple) and tripartite (blue) (A) *Comamonas testosteroni*, (B) *Nitrosomonas europaea* and (C) *Nitrobacter winogradskyi*. COG classes 'Function unknown' and 'General function prediction only' were excluded.

in the five highest ranked COGs in both cultures. Respectively 36.62% and 34.78% of all DEGs could not be annotated to a specific COG class for the axenic and tripartite culture. Only one common DEG (NE1243), coding for a hypothetical protein, was identified in both conditions.

'Translation, ribosomal structure and biogenesis' (Axenic: 4.55%, Tripartite: 3.92%), 'Inorganic ion transport and metabolism' (Axenic: 4.55%, Tripartite: 7.84%) and 'Transcription' (Axenic: 4.55%, Tripartite: 7.84%) overlapped in the top five most affected COGs in axenic and tripartite *N. winogradskyi* (Figure 4C). For the axenic culture, 31.81% of DEGs could not be annotated to a specific COG while this number was 24.51% for the tripartite culture. Two overlapping DEGs (NITWN7139, NITWN7140) both coding for hypothetical proteins were identified.

Impact of IR exposure on ureolysis- and nitrification-related genes

No ureolysis genes were differentially regulated in both axenic and tripartite *C. testosteroni* after IR exposure. However, in the pure culture, the gene coding for arginase (*rocF*; JMRS01_600033), which converts arginine to urea and ornithine, was upregulated. Nitrate transport protein (*nasD*; JMRS01_700263) and nitric oxide detoxification (*hmp*; JMRS01_600263, *norR1*; JMRS01_600264) gene expression was also induced. Nitrification genes were unaffected in axenic *N. europaea* and in axenic and tripartite *N. winogradskyi* cultures. However, in

N. europaea in the tripartite culture, we observed inhibition of expression of nitrite reductase-coding gene *nirK* (NE0924) and one of its accessory genes *ncgC* (NE0925). Meanwhile, expression of hydroxylamine oxidoreductase-coding gene *hao* (NE2339), responsible for the second step of NH_4^+ oxidation, increased in the tripartite culture.

Differential expression of stress response and DNA repair genes after IR exposure

Transcripts of only one gene involved in direct ROS scavenging, coding for a putative alkylhydroperoxidase (JMRS01_810045), were detected in increased levels in axenic *C. testosteroni* samples. In *C. testosteroni* in the tripartite configuration, gene expression of disulfide bond formation protein B (*dsbB*; JMRS01_150035), related to disulfide bond formation and repair in periplasmic proteins,[17] strongly increased with an FC of 33.22. Alkylhydroperoxide reductase subunit-coding genes *ahpF/C* (JMRS01_400034/5) also demonstrated enhanced transcriptional activity and are responsible for scavenging H_2O_2 molecules.[18] Transcription of the GroEL/ES complex (*groES/groEL*; JMRS01_700212/3), chaperone protein HtpG (*htpG*; JMRS01_600186), protease HtpX (*htpX*; JMRS01_600027), involved in stabilization or degradation of proteins damaged by oxidation, and a universal stress protein-coding gene (JMRS01_760025) were all promoted in the tripartite culture. In both *C. testosteroni* configurations, DNA repair machinery was differentially regulated. In the axenic culture, expression of DNA repair genes *xseB* (JMRS01_50018) *radC* (JMRS01_220071), *mutS* (JMRS01_220072), *recD* (JMRS01_340049) and 8-oxoguanine deaminase-coding gene *atzB* (JMRS01_260149) was promoted. In its tripartite counterpart, formamidopyrimidine-DNA glycolase (*mutM*; JMRS01_700030) and *recX* (JMRS01_360198) were upregulated.

A limited amount of stress response-related genes were affected in *N. europaea*. Only *groES/groEL* (NE0027/28) expression significantly increased in the pure strain while no stress response genes were differentially expressed in *N. europaea* in the tripartite configuration.

Finally, catalase-peroxidase-coding gene *katG* (Nwi_0030), of which the protein detoxifies H_2O_2 molecules, was strongly upregulated (FC = 4.96) in axenic *N. winogradskyi*. Also, putative carboxymuconolactone decarboxylase (Nwi_0460) expression increased and has been implicated as an important catalyst in the production of aromatic antioxidants in *Corynebacterium glutamicum*.[19] Hence, it possibly plays a role in the oxidative stress response. Surprisingly, several proteins putatively involved in stress response were inhibited. These include putative cold shock protein (Nwi_1609), heat shock protein (Nwi_2936) and non-homologous end-joining (NHEJ) DNA repair protein LigD (Nwi_0353). In the tripartite culture, chaperone protein-coding genes *clpB* (Nwi_0589), *groL2* (Nwi_2192) and *groL3* (Nwi_2574) and a HSP20-coding gene (Nwi_1115) were overexpressed by *N. winogradskyi*. On the other hand, but not unlike axenically grown *N. winogradskyi*, we observed decreased expression of a gene coding for putative cold shock protein (Nwi_1599). Unexpectedly, putative alkyl hydroperoxide reductase- and peptide methionine sulfoxide reductase-coding genes (Nwi_0891 and *msrA*; Nwi_0971, respectively) were also downregulated. These proteins are respectively involved in detoxification of ROS and repair of proteins damaged by oxidation.

Metal ion homeostasis is adapted in response to low-dose IR

Changes in the transcription of genes involved in heavy metal secretion and chelation, which could reduce ROS load, were observed across all species after IR exposure. In axenic *C. testosteroni*, periplasmic copper chaperone A (JMRS01_340044), copper efflux regulator (*cueR*; JMRS01_360154), a heavy metal response transcriptional regulator (JMRS01_600253) and a heavy metal efflux system membrane fusion protein (JMRS01_860361) displayed increased transcript levels. Iron import gene expression was decreased, reflected in reduced expression of genes involved in iron-siderophore uptake such as ExbB (JMRS01_10042), ExbD (JMRS01_730014), and putative TonB-dependent receptor protein FecA (JMRS01_10043). FecA receptors are part of FecARI iron-siderophore import machinery, which governs iron siderophore import in response to the extracellular presence of those complexes.[20] In the tripartite culture, the inhibition of two *fecA* genes (JMRS01_600118, JMRS01_1030018) and upregulation of a bacterioferritin-coding gene (*bfr*; JMRS01_400036) was observed. Meanwhile, expression of a heavy metal outer membrane (OM) efflux protein CzcC (JMRS01_390046) was inhibited, but putative heavy metal response transcriptional regulator (JMRS01_150006) expression increased.

From a perspective of iron homeostasis, *N. europaea* was the most affected strain. In the axenic culture, several genes putatively belonging to FecARI systems were differentially expressed (Table 2). A gene coding for a multicopper oxidase (*mnxG*; NE0315) was downregulated after IR exposure while an OM efflux protein CzcC-coding gene (NE1640) was upregulated. No FecARI systems were affected in *N. europaea* in the tripartite culture. However, some heavy metal homeostasis genes were differentially regulated. An OM efflux protein-coding gene (NE0373) was downregulated, and expression of transcriptional co-regulator *merD* (NE0838), linked to the negative transcription of the *mer*-operon (NE0839 – NE842) in response to decreased intracellular Hg pools,[21] increased. The *mer*-operon, however, was not differentially expressed.

Finally, while no heavy metal homeostasis genes in axenic *N. winogradskyi* were differentially regulated, downregulation of three putative FecA-coding genes (Nwi_0253, Nwi_0700, Nwi_0941), 2 *fecI*-like genes (Nwi_2303, Nwi_2883) and putative bacterioferritin-coding gene (*bfr*; Nwi_2476) was observed in the tripartite culture.

Sulfate import and assimilation gene modulation in response to IR exposure

The sulfur metabolism also seemed to be an important factor in the IR exposure response. Genes of the CysUWA ATP-dependent sulfate import system were upregulated in both axenic and tripartite *C. testosteroni*. More specifically, transcription of *sbp* (substrate-binding protein) (JMRS01_150031) and *cysA* (JMRS01_150031/34) for the axenic culture, and *cysW* (JMRS01_150033) for the tripartite culture increased. Moreover, in the pure *C. testosteroni* culture, the sulfate assimilation-related gene cluster JMRS01_10006 – 10010 (*cysNDHI* and a hypothetical gene) expression was upregulated. In axenic *N. europaea*, a sulfate import and assimilation gene cluster (NE0572 – NE0583) was also

Table 2. Overview of differentially expressed iron acquisition genes in axenic *Nitrosomonas europaea* cultures after exposure to ionizing radiation

GeneID	Gene name	Description	Fold Change
Upregulated iron uptake genes			
NE0636	*fecA*	TonB-dependent receptor protein	2.06
Downregulated iron uptake genes			
NE0730	*Fur*	Ferric uptake regulation family protein	−2.18
NE0754	*fecA*	TonB-dependent receptor	−2.06
NE0980	*fecI*	ECF subfamily RNA polymerase sigma-70 factor	−2.30
NE1070	*fecR*	transmembrane sensor	−2.10
NE1071	*fecI*	ECF subfamily RNA polymerase sigma-70 factor	−2.35
NE1079	*fecI*	ECF subfamily RNA polymerase sigma-70 factor	−2.17
NE1099	*fecI*	ECF subfamily RNA polymerase sigma-70 factor	−2.79
NE1101	*fecI*	ECF subfamily RNA polymerase sigma-70 factor	−2.62
NE1217	*fecI*	ECF subfamily RNA polymerase sigma-70 factor	−2.28
NE1540	*fecA*	TonB-dependent receptor protein	−2.33
NE1617	*fecI*	ECF subfamily RNA polymerase sigma-70 factor	−2.58
NE1618/NE1619[a]	*fecR*	Transmembrane sensor	−2.71/-1.84
NE2124	*fecA*	TonB-dependent receptor protein	−2.97
NE2435	*fecI*	ECF subfamily RNA polymerase sigma-70 factor	−3.18

[a]Gene sequence of NE1618/NE1619 contains a premature stop codon and could be a pseudogene.

upregulated. In addition to CysUWA, serine O-acetyltransferase (NE0575), involved in cysteine and methionine biosynthesis, a CysB-like protein (*cbl*; NE072), which is a transcriptional regulator in response to sulfate starvation, and a cysteine desulfurase (*sufS*; NE0573) gene are contained in the cluster. No sulfur metabolism-related genes were differentially expressed in the tripartite culture for *N. europaea*. In *N. winogradskyi* in the tripartite culture, the downregulation of genes coding for putative Fe-S cluster assembly proteins (Nwi_1659, Nwi_1809) and for cysteine desulfurase (*iscS*; Nwi_1665) was observed while sulfur metabolism-related gene expression of axenic *N. winogradskyi* was unaffected.

Central metabolic pathway gene regulation in response to IR in axenic *C. testosteroni*

Genes coding for citryl-CoA lyase (*citE*; JMRS01_560035) and malate dehydrogenase (*mdh*; JMRS01_560037) were induced. These proteins respectively catalyze the second step in the cleavage of citrate to oxaloacetate and acetyl-CoA, and the reversible conversion of malate to oxaloacetate. Transcription of a gene coding for a key component of the glyoxylate shunt (GS), isocitrate lyase (*aceA*; JMRS01_10058) increased. Glycolate dehydrogenase (*glcE*; JMRS01_350057), which converts glycolate to glyoxylate, was also overexpressed. Acetyl-CoA production genes coding for acetate kinase (*ackA*; JMRS01_540010), phosphate acetyltransferase (*pta*; JMRS01_540011) and malate:quinone oxidoreductase (*mqo*; JMRS01_860295) were also overexpressed in axenic *C. testosteroni*. Meanwhile, no signs of GS activation were observed in *C. testosteroni* in the tripartite culture, but the downregulation of 2 genes (*glcF*; JMRS01_350058, *hyi*; JMRS01_860370) involved in glyoxylate biosynthesis was observed. In *N. europaea* and *N. winogradskyi*, tricarboxylic acid (TCA) cycle and GS genes were not affected.

IR-induced DGE involved in cell envelope stability and membrane integrity

Axenic *C. testosteroni* displayed DGE of several genes that code for proteins involved in producing and transporting membrane and cell wall constituents. Genes coding for putative inner membrane protein ElaB (JMRS01_190079), putative fatty-acyl CoA synthase (JMRS01_400011), glycerol-3-phosphate dehydrogenase (*gspA*; JMRS01_260006), CreD (JMRS01_700026), putative OM lipoprotein (JMRS01_700143), phospholipid transport-binding protein (JMRS01_700150) and operon JMRS01_380058 – JMRS01_380064, which includes cyclopropane fatty acyl phospholipid synthase (*cfa*; JMRS01_380060), were upregulated. Moreover, expression of a lytic transglycosylase gene

(JMRS01_700081) and N-acyl-D-amino acid deacylase-coding gene (JMRS01_320181), with roles in cell wall synthesis and remodeling[22,23] increased.

In *C. testosteroni* in the tripartite culture, other DEGs with roles in cell envelope stabilization and alteration were identified. Genes coding for an OM lipoprotein (*blc*; JMRS01_310044), fatty acid biosynthesis genes S-malonyltransferase (*fabD*; JMRS01_60013), putative fatty acid desaturase (JMRS01_1050089), cardiolipin synthase A/B (*clsA/B*; JMRS01_650076), hyperosmotically inducible periplasmic protein (*osmY*; JMRS01_650097) and PG-associated OM lipoprotein Pal (*pal*; JMRS01_1030049) were all upregulated.

Limited DGE related to the cell envelope was observed in axenic *N. europaea*. Downregulation of a gene cluster (NE2347 – NE2350) containing a major facilitator superfamily (MFS) transporter (NE2347), an acyl-CoA dehydrogenase (*fadE1*; NE2348), a putative acyl-CoA synthetase (*ydiD*; NE2349) and a putative acyl-CoA transferase (NE2350), was observed. No DEGs with related functions were identified in the tripartite counterpart.

Finally, *N. winogradskyi* did not display any DGE in the axenic configuration. Still, in the tripartite culture, gene expression of a glycosyltransferase (Nwi_0326) and cell envelope biogenesis protein AsmA (Nwi_1009) increased while expression of UDP-3-*O*-acylglucosamine N-acyltransferase (*lpxD2*; Nwi_3100) decreased.

DISCUSSION

Radiotolerance and growth kinetics of N-cycle bacteria after exposure to IR

C. testosteroni and *N. europaea* exhibited growth after exposure to D_T-values of at least 400 Gy, while a total dose between 200 and 400 Gy seemed sufficient to completely sterilize *N. winogradskyi* cultures. Activity tests of *N. europaea* and *N. winogradskyi* also confirmed the strains to be active after 200 Gy of irradiation. In both cases, no activity was observed after exposure of 400 Gy of irradiation upwards although growth was observed in *N. europaea* cultures. These results could indicate a highly delayed onset of NH_4^+ oxidation after 400 Gy of irradiation. Finally, caution should be taken when interpreting data from *N. winogradskyi*. Evaporation in certain sample wells of *N. winogradskyi* cultures caused a concentration of compounds in the wells, resulting in very large standard deviations and a bias toward higher NO_2^- measurements. The D_{10}-value of 87.99 $\pm$ 1.21 Gy determined for *C. testosteroni* is, to our knowledge, the first to be reported for this strain. We were unable to determine a D_{10}-value for *N. europaea* and *N. winogradskyi* using EAC measurements. The used kit seemed unable to lyse *N. winogradskyi* cells while in *N. europaea* cultures, metabolically active cells were detected by EAC determination at even the highest doses of irradiation. One should be cautious interpreting the results as we expect no viable cells at very high D_T, considering the results from growth curve and activity experiments. It is possible that non-viable but non-lysed cells still possess intracellular ATP, so measured intracellular ATP concentration could not be used to exactly determine the amount of EAC and thus viability for *N. europaea*.

In general, the reported values of the growth kinetics and the D_{10}-value of *C. testosteroni* are low compared to other bacteria. For example, a study on radiosensitive bacteria *Escherichia coli* and *Staphylococcus epidermidis* completely sterilized the strains after 4,000 Gy of γ-irradiation.[24] Meanwhile, D_{10}-values reported for *E. coli* range from 200 Gy to 650 Gy[24,25] while a similar D_{10}-value to *C. testosteroni* of 70 Gy has been determined for *Shewanella oneidensis*, which is considered a radiosensitive strain.[26,27] However, recovery from IR exposure also depends on culturing medium, pH and other growth conditions.[28] In this study, *C. testosteroni* was grown in minimal SUSS medium but might respond better to IR in a richer medium, providing ameliorated growth conditions and anti-oxidative protection. The same can be said for the nitrifiers when grown in optimized media like ATCC 2265 for *N. europaea* or DSMZ-756 for *N. winogradskyi* instead of the synthetic urine-like alternative used in this study.

Lag time (λ) of the strains exposed to acute IR increased with increasing radiation doses, which was also observed previously with the effect of UV-radiation or IR on growth kinetics of *E. coli*, *Pseudomonas aeruginosa* and *Salmonella typhimurium*.[29,30] Bacterial cultures that experienced a variety of stresses that result in sublethal injuries often exhibit increased lag times.[31] Consequently, the duration of the lag time could be viewed as a representation of sublethal damaged cells and the amount of surviving bacteria after IR.

After exposure to low-dose ISS-like IR throughout its exponential growth phase, significantly higher OD_{600} values for axenic *C. testosteroni* were observed. On the other hand, the relative distribution of the bacterial strains within the tripartite culture was not affected by low-dose IR exposure and no significant difference in the OD_{600} measurement of the synthetic community was measured. Consequently, we could also conclude that low-dose IR did not have an effect on the measured cell density of *C. testosteroni* in the tripartite culture. In this configuration, *C. testosteroni* was already in stationary phase. Combined, these observations could imply that cell proliferation in the exponential phase was enhanced for *C. testosteroni* by low-dose IR. However, additional research should be conducted to confirm this. Proliferation of the axenic nitrifiers and their abundance in the tripartite culture were unaffected by low-dose IR.

Global whole transcriptome changes in N-cycle bacteria exposed to low-dose IR

The effects on gene expression of the different strains in either pure or tripartite configuration differ from strain to strain and from culture setup to culture setup. Low-dose IR causes transcriptomic changes in response to increased ROS-load due to the interaction of IR with H_2O molecules in the bacteria. These increased ROS loads influence a variety of cellular processes, and similar processes were affected from a transcriptomic point of view in different strains in the axenic and tripartite configurations. A high-level overview of recurring impacted cellular processes across different strains after exposure to low-dose IR is provided in Figure 5.

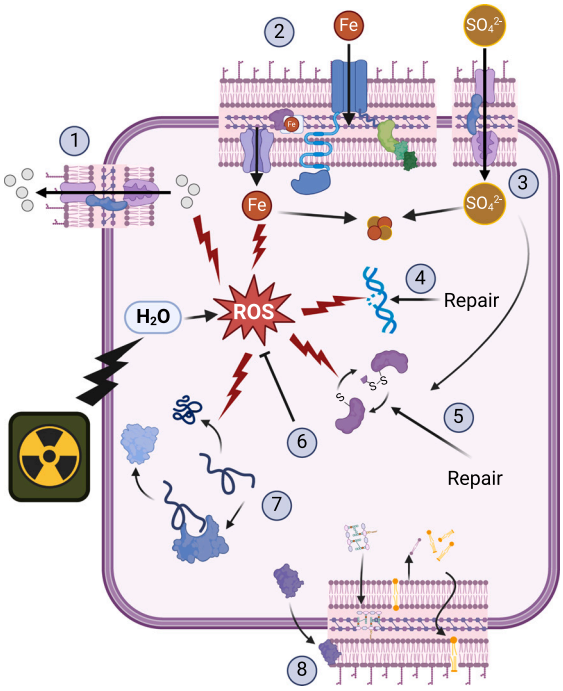

		Comamonas testosteroni		*Nitrosomonas europaea*		*Nitrobacter winogradskyi*	
		Axenic	Tripartite	Axenic	Tripartite	Axenic	Tripartite
1	Heavy metal ion export	↑	↑↓	↑	↓	ND	↓
2	Fe^{2+} import	↓	↓	↓	ND	ND	↓
3	Sulfate metabolism	↑	↑	↑	ND	↓	ND
4	DNA repair	↑	↑	ND	ND	↓	ND
5	Protein repair	ND	↑	ND	ND	ND	↓
6	ROS detoxification	↑	↑	ND	ND	↑	↓
7	Chaperones	ND	↑	↑	ND	↓	↑↓
8	Cell envelope	↑↓	↑↓	↑↓	ND	ND	↑↓

Figure 5. Overview of transcriptomic changes in N-cycle bacteria exposed to low-dose ionizing radiation (IR)

(1) Increased reactive oxygen species (ROS) load can be diminished by regulating the export of ROS-generating heavy metal ions. (2) The import of Fe^{2+} ions can increase ROS load through the Fenton-reaction. (3) Import of sulfate, which can be used for Fe-S cluster assembly and for oxidative stress response mechanisms. (4) The repair of DNA damaged by ROS. (5) The repair of proteins damaged by ROS. (6) ROS detoxification mechanisms. (7) Chaperone proteins that prevent misfolding of polypeptides damaged by ROS. (8) Adaptations to the cell envelope. Green arrows indicate upregulation of process-related genes while red arrows indicate downregulation. ND means no differential expression has been observed for that category in the bacterial strain.

Minimal impact on ureolysis and nitrification gene transcription after low-dose IR exposure

Most importantly, urea hydrolysis and nitrification genes were mostly unaffected after exposure to low-dose chronic IR. In *N. europaea*, *nirK* expression was inhibited in the tripartite culture. NirK is important during NH_4^+ oxidation by decreasing NO_2^- accumulation and toxicity through denitrification.[32] In the tripartite culture after exposure to IR, this downregulation could be a mechanism to reduce reactive nitrogen species (RNS) production by diminishing the capacity to reduce NO_2^- to NO, which can eventually generate RNS.[33] Hence, one could hypothesize that this gene expression pattern was the result of a preference to slightly increased NO_2^- toxicity over production of additional RNS. Moreover, due to the presence of *N. winogradskyi* in the synthetic community, *N. europaea* could have been able to afford this, given the former's NO_2^- oxidation capacities to effectively diminish NO_2^- concentrations. In axenic *C. testosteroni*, the upregulation of nitric oxide detoxification genes *hmp* and *norR1* could imply a mechanism to combat oxidative (and nitrosative) stress.[34] Meanwhile, *rocF* has been suggested to reduce RNS generation in *Helicobacter pylori* by inhibiting NO production through the consumption of arginine[35] and potentially serves a similar function in *C. testosteroni* after exposure to low-dose IR.

Low-dose IR has a nuanced impact on the gene expression of stress response genes

N. europaea exhibited the least amount of DEGs coding for ROS detoxification and general stress response proteins, while *C. testosteroni*, particularly in the tripartite culture, displayed the highest responsiveness. DNA repair mechanisms and chaperones like the GroES-GroEL system, a heat shock protein complex known to be induced in stress conditions to avoid protein aggregation and misfolding,[36] were most commonly upregulated across strains. However, the expression of DNA repair-related genes was ambiguous across the strains. For example, in axenic *N. winogradskyi*, NHEJ DNA repair protein-coding gene *ligD* was downregulated. Meanwhile, genes involved in DNA repair mechanisms were upregulated in *C. testosteroni* in the axenic and tripartite culture. These genes include *xseB*, *radC*, *mutS*, *recD* and *atzB* in pure *C. testosteroni* cultures. All these genes play a direct or indirect role in DNA repair after damage caused by ROS. Some are more nuanced than others. In particular, AtzB deaminates 8-oxoguanine (oxoG) molecules to uric acid. OxoG is a product of ROS interaction with guanine residues within DNA which, in turn, results in C:G to A:T transversions. These oxoG molecules can be excised but have to be deaminated to prevent reincorporation of this compound in DNA and are active under increased ROS presence.[37] On the other hand, in the tripartite configuration, *C. testosteroni* increased expression of *mutM* but also of *recX*, which inhibits RecA homologous DSB repair activity.[38] Across the bacterial strains, however, there is no clear evidence that low-dose IR induced DNA strand breaks, an observation that was also made in *E. coli* when exposed to different types of low-dose IR.[39]

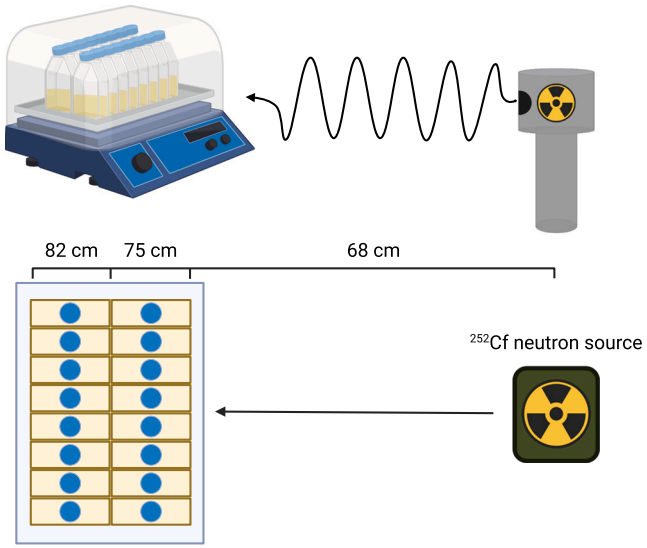

Figure 6. Schematic overview of the experimental setup during low-dose chronic irradiation with a pure neutron source (Cf-252)

In general, the ROS burden generated by low-dose irradiation appears to be limited, reflected in the sparse amount of DEGs with roles in ROS detoxification mechanisms, with some genes even showing downregulation. Similarly, a recent transcriptome analysis on *E. coli* exposed to a low-dose of IR from diverse sources also revealed that changes in gene expression were not predominantly associated with stress responses and gene expression was also inhibited in some conditions.[39] Hence, the response to low-dose IR exposure is more nuanced than a general upregulation of oxidative stress response and DNA repair machinery, as is usually the case after exposure to high-dose IR.[27,39]

Iron and sulfate metabolism are important in response to low-dose IR

Across all species, gene expression related to iron homeostasis was impacted. For one, axenic and tripartite *C. testosteroni*, axenic *N. europaea* and tripartite *N. winogradskyi* all decreased expression of iron uptake and sequestration genes. A decrease in iron acquisition genes could reduce the intracellular free Fe^{2+} pool and thereby attenuate the generation of $^{\cdot}OH$ radicals in the Fenton reaction.[15,40] The most prominent effect of IR on bacterial iron homeostasis was observed in *N. europaea*. The gene expression of 1 Fur family protein (NE0730) out of three in the *N. europaea* genome, was inhibited. In a previous spaceflight experiment with *Rhodospirillum rubrum*, the gene was found to be significantly upregulated, but it signifies that this gene's regulation could be involved in the bacterial response to IR.[41] The *fur*-gene is almost certainly an important factor in the iron uptake mechanism of *N. europaea*, since it was also upregulated 15-fold in iron starvation conditions.[42] All *fecI* DEGs were also upregulated during iron starvation,[42] which consequently implicates the induction of expression of the remaining *fecA* and *fecR* genes.[43] The role of iron acquisition genes but also of *mnxG* in the response to oxidative stress in *N. europaea* was also apparent in a study on heavy metal exposure. Here, *mnxG* and *fecARI* genes (NE0636, NE0730, NE1217 and NE2435) were downregulated and suggest a role in alleviating oxidative stress.[44,45] Considering the significance of iron homeostasis in the metabolism of *N. europaea*, reflected in the large amount of genes involved in iron-siderophore uptake, heme synthesis and Fe-S cluster generation in its genome,[46,47] strict regulation of intracellular Fe^{2+} levels to combat oxidative stress could be a valuable strategy for *N. europaea* in response to IR. However, this was not observed in *N. europaea* in the tripartite culture. Here, only the expression of the *mer*-operon regulator increased, which was also observed during heavy metal exposure.[44] DGE of the *merD* gene in both heavy metal exposure and IR in this study could indicate its involvement in a response to oxidative stress.

Increased expression of sulfur import and assimilation genes in axenic and tripartite *C. testosteroni* and axenic *N. europaea* infer a role of these mechanisms in response to IR. These genes are important in Fe-S cluster biosynthesis and the cysteine and methionine metabolism and highlight the importance of an expanded sulfur pool during low-dose IR exposure. For example, cysteine desulfurase (SufS), involved in Fe-S cluster biosynthesis,[48] has been induced in oxidative stress conditions in previous studies.[49] Excess iron is often incorporated in Fe-S clusters[50] and could be an additional strategy to limit free intracellular Fe^{2+} levels during oxidative stress. Meanwhile, additional sulfur could also serve to regenerate damaged sulfur-containing cysteine and methionine residues. Additionally, cysteine serves as an important precursor in glutathione biosynthesis, an important ROS detoxification protein. On the other hand, in *N. winogradskyi* in the tripartite culture, sulfur assimilation and Fe-S cluster biosynthesis-related gene expression was inhibited and seemed to point at a decrease in Fe-S cluster biosynthesis. Hence, the role of sulfur assimilation in response to low-dose IR varies across species.

Low-dose IR triggers metabolic reprogramming in *Comamonas testosteroni*

Another indication of oxidative stress caused by low-dose IR was observed in axenic *C. testosteroni* with the upregulation of the GS machinery. DGE of GS-related genes has already been implicated in the oxidative stress response in several bacteria.[51,52] The GS bypasses two NADH-producing decarboxylation steps in the TCA, allowing bacteria to use 2-carbon compounds such as acetate more efficiently and increasing flux toward anabolic pathways such as gluconeogenesis.[53] By increasing GS activity during oxidative stress, NADH production is attenuated, retarding ROS-generating reactions in the electron transport chain. The upregulation of *ackA* and *pta* in axenic *C. testosteroni* cultures may be another example of the reprogramming of metabolic networks during oxidative stress. These genes catalyze the reversible production of acetate from pyruvate. In the presence of ROS, pyruvate can undergo non-enzymatic decarboxylation, producing acetate and detoxifying ROS in the process.[53] Increased expression of these genes thus suggests heightened activity of the acetate metabolism to enhance cycling between pyruvate and acetate. In the tripartite culture, no GS-related genes were affected and the downregulation of *glcF* and *hyi* suggested that flux toward the GS is not increased.

Expression of cell envelope genes of N-cycle bacteria is affected by low-dose IR

Finally, the induction of genes involved in maintaining cell envelope stability and membrane integrity in *C. testosteroni* in both the axenic and tripartite configuration was observed. *Cfa*, *elaB*, and *creD*, upregulated in pure *C. testosteroni* cultures, have been reported to function in maintaining membrane stability and integrity during stressful conditions[54–56] and could consequently be involved in the response to low-dose IR. DGE of related genes in *N. europaea* and *N. winogradskyi* were limited but nonetheless also present. All reported DEGs can be linked to cell envelope restructuring and maintenance. Hence, low-dose IR also induced changes in expression of cell envelope-related genes.

Age-related differences and interspecies dynamics influence gene expression of N-cycle bacteria

Although not many overlapping DEGs were identified in axenic strains of *C. testosteroni*, *N. europaea* and *N. winogradskyi* compared to their tripartite counterparts, similar cellular processes were often affected. The differences in gene expression profiles between the axenic and tripartite culture strains could be a consequence of the age of the cultures, a phenomenon previously observed in *E. coli* after IR exposure.[39] For example, axenic *C. testosteroni* was 3 days old after the low-dose IR exposure while the tripartite strain was 23 days old after that time period. DEGs involved in stress response identified in axenic *C. testosteroni* and tripartite *C. testosteroni* were different but the transcriptomic profile pointed at an increased oxidative stress response in both cases. Apart from age-related differences, variations in gene expression of bacteria in axenic cultures and in co-culture often arise due to interspecies dynamics.[57,58] Which interspecies dynamics exert which effects on gene expression requires further exploration. However, the findings presented in this study do allow for the formulation of some hypotheses. For one, *N. europaea*'s differential transcription of *nirK* in the tripartite culture could be an effect of diminished NO_2^- concentrations in the tripartite culture due to the presence of the NO_2^--oxidizing *N. winogradskyi*. In addition, DGE was nearly ubiquitous for genes involved in the efflux of heavy metals, as shown in Figure 5. Which heavy metal ions were targeted and if the heavy metal efflux system genes were up- or downregulated was not consistent. However, heavy metal ion efflux plays an important role in alleviating increased ROS loads. In some cases, reducing the concentration of a certain heavy metal ion in the cell can result in reduced redox cycling and thereby reduced ROS generation. Another method of combating ROS loads is by introducing metal ions such as Mn^{2+} or Zn^{2+} to displace Fe^{2+} from sensitive targets.[59] The bacterial strain and its co-occurrence with other bacteria could influence which metal ion homeostasis functions are impacted during low-dose IR exposure. Finally, *C. testosteroni* and *N. europaea* seem to be less susceptible to low-dose IR in a tripartite community while *N. winogradskyi* displayed a higher degree of DGE compared to its axenic counterpart. However, this interpretation should be taken with caution given the disparity between total CDS and mapped CDS for *C. testosteroni* and *N. winogradskyi* in the tripartite culture.

Overall, the results presented in this study indicate that *C. testosteroni* I2, *N. europaea* ATCC 17918 and *N. winogradskyi* Nb-255 can be considered radiosensitive bacterial strains, which also suggests susceptibility to low-dose IR. Meanwhile, the effects of low-dose IR on the transcriptome of the bacteria revealed a limited impact on the cellular physiology. This analysis broadens our current knowledge of the impact of low-dose IR on bacteria and sheds light on how spaceflight could affect the bacterial metabolism. The gene expression profiles of MELiSSA's CIII urine nitrification strains suggest a diverse transcriptional response that can differ from species to species. In particular, gene expression related to ureolysis and nitrification, both critical processes in the recovery of nitrogen from urine and other waste streams, remained mostly unaffected.

Limitations of the study

This study is accompanied by some limitations. Although we were able to establish hypotheses of the effects of low-dose IR on the bacterial strains using transcriptomic profiling, they should be validated by other research to assess if these gene expression variations translate to a proteomic and phenotypical level. Additionally, our model to simulate ISS-like IR does not account for the effects of other types of radiation present on board of the ISS. As discussed, various radiation types elicit distinct transcriptomic effects.[39] For this study, we chose the radiation source that generates neutron radiation, which is the most common on board

the ISS.[7] Moreover, by choosing an accelerated-life experimental setup, which implicated higher dose rates, the effects that we observed are likely amplified in comparison to real spaceflight radiation. Finally, this study only accounts for the short-term effects of the IR environment of space. The influence of chronic exposure to space IR over a multigenerational time span could induce other mechanisms that were not observed in this study.

STAR★METHODS

Detailed methods are provided in the online version of this paper and include the following:

- KEY RESOURCES TABLE
- RESOURCE AVAILABILITY
  - Lead contact
  - Materials availability
  - Data and code availability
- EXPERIMENTAL MODEL AND SUBJECT DETAILS
  - Microbial strains
- METHOD DETAILS
  - Determination of radiotolerance of axenic cultures
  - OD_{600} measurements
  - Analysis of growth after acute irradiation
  - Colony-forming unit (CFU) determination
  - Intracellular ATP measurement
  - Activity testing
  - ISS-like low-dose irradiation
  - Relative abundance of strains in the tripartite community
  - RNA extraction
  - RNA sequencing
  - RNA-Seq data analysis
  - Data visualization
- QUANTIFICATION AND STATISTICAL ANALYSIS

SUPPLEMENTAL INFORMATION

Supplemental information can be found online at https://doi.org/10.1016/j.isci.2024.109596.

ACKNOWLEDGMENTS

This work was part of the URINIS-A project, funded by the Belgian Federal Science Policy Office (BELSPO; Contract # PEA 4000129030) and ESA via the PRODEX program. The URINIS-A project is part of the MELiSSA program of ESA, ESA's life support system development program (www.melissafoundation.org). RG was supported by the Special Research Fund of Ghent University [BOF19/STA/044]. The authors thank Dr. Mohamed Mysara for his valuable support on the RNA-Seq analysis, Rob Van Houdt for his resourceful advice on the qPCR workflow, Olivier Van Hoey for his assistance in the selection of a proper radiation source for the space-analogue radiation and Hugo Moors for his help with the modeling of growth curves for the determination of growth kinetics.

AUTHOR CONTRIBUTIONS

Conceptualization: T.V., B.L., N.L., R.G., and F.M.; Methodology: T.V. and F.M.; Software: T.V. and S.G.; Formal analysis: T.V. and S.G.; Investigation: T.V., C.A.F., T.H.N., and F.M.; Writing – Original draft: T.V. and F.M.; Writing – Review and editing: T.V., C.A.F., T.H.N., B.L., R.W., S.E.V., N.L., R.G., and F.M.; Funding acquisition: N.L., R.G., S.E.V., and F.M.; Supervision: N.L., R.G., and F.M.

DECLARATION OF INTERESTS

The authors declare no competing interests.

Received: January 19, 2024
Revised: February 8, 2024
Accepted: March 25, 2024
Published: March 27, 2024

REFERENCES

1. Hendrickx, L., De Wever, H., Hermans, V., Mastroleo, F., Morin, N., Wilmotte, A., Janssen, P., and Mergeay, M. (2006). Microbial ecology of the closed artificial ecosystem MELiSSA (Micro-Ecological Life Support System Alternative): reinventing and compartmentalizing the Earth's food and oxygen regeneration system for long-haul space exploration missions. Res. Microbiol. *157*, 77–86. https://doi.org/10.1016/j.resmic.2005.06.014.
2. Lasseur, C., Brunet, J., De Weever, H., Dixon, M., Dussap, G., Godia, F., Leys, N., Mergeay, M., and Van Der Straeten, D. (2010). MELiSSA: The European Project of a Closed Life Support System. Gravitational Space Biol. *23*, 3–12.
3. Ilgrande, C., Defoirdt, T., Vlaeminck, S.E., Boon, N., and Clauwaert, P. (2019). Media Optimization, Strain Compatibility, and Low-Shear Modeled Microgravity Exposure of Synthetic Microbial Communities for Urine Nitrification in Regenerative Life-Support Systems. Astrobiology *19*, 1353–1362. https://doi.org/10.1089/ast.2018.1981.
4. Vanhavere, F., Genicot, J.L., O'Sullivan, D., Zhou, D., Spurný, F., Jadrníčková, I., Sawakuchi, G.O., and Yukihara, E.G. (2008). DOsimetry of Blological EXperiments in SPace (DOBIES) with luminescence (OSL and TL) and track etch detectors. Radiat. Meas. *43*, 694–697. https://doi.org/10.1016/j.radmeas.2007.12.002.
5. Dachev, T., Horneck, G., Häder, D.P., Schuster, M., and Lebert, M. (2015). EXPOSE-R cosmic radiation time profile. Int. J. Astrobiol. *14*, 17–25. https://doi.org/10.1017/S1473550414000093.
6. Kodaira, S., Naito, M., Uchihori, Y., Hashimoto, H., Yano, H., and Yamagishi, A. (2021). Space Radiation Dosimetry at the Exposure Facility of the International Space Station for the Tanpopo Mission. Astrobiology *21*, 1473–1478. https://doi.org/10.1089/ast.2020.2427.
7. Berger, T., Przybyla, B., Matthiä, D., Reitz, G., Burmeister, S., Labrenz, J., Bilski, P., Horwacik, T., Twardak, A., Hajek, M., et al. (2016). DOSIS & DOSIS 3D: long-term dose monitoring onboard the Columbus Laboratory of the International Space Station (ISS). J Space Weather Spac *6*, A39. https://doi.org/10.1051/swsc/2016034.
8. Krukowski, K., Grue, K., Becker, M., Elizarraras, E., Frias, E.S., Halvorsen, A., Koenig-Zanoff, M., Frattini, V., Nimmagadda, H., Feng, X., et al. (2021). The impact of deep space radiation on cognitive performance: From biological sex to biomarkers to countermeasures. Sci. Adv. *7*, eabg6702. https://doi.org/10.1126/sciadv.abg6702.
9. Siasou, E., Johnson, D., and Willey, N.J. (2017). An Extended Dose Response Model for Microbial Responses to Ionizing Radiation. Front. Environ. Sci. *5*. https://doi.org/10.3389/fenvs.2017.00006.
10. Moeller, R., Raguse, M., Leuko, S., Berger, T., Hellweg, C.E., Fujimori, A., Okayasu, R., and Horneck, G.; the STARLIFE Research Group (2017). STARLIFE-An International Campaign to Study the Role of Galactic Cosmic Radiation in Astrobiological Model Systems. Astrobiology *17*, 101–109. https://doi.org/10.1089/ast.2016.1571.
11. Verbeelen, T., Leys, N., Ganigué, R., and Mastroleo, F. (2021). Development of Nitrogen Recycling Strategies for Bioregenerative Life Support Systems in Space. Front. Microbiol. *12*, 700810. https://doi.org/10.3389/fmicb.2021.700810.
12. Moeller, R., Reitz, G., Berger, T., Okayasu, R., Nicholson, W.L., and Horneck, G. (2010). Astrobiological Aspects of the Mutagenesis of Cosmic Radiation on Bacterial Spores. Astrobiology *10*, 509–521. https://doi.org/10.1089/ast.2009.0429.
13. Dartnell, L.R., Desorgher, L., Ward, J.M., and Coates, A.J. (2007). Modelling the surface and subsurface Martian radiation environment: implications for astrobiology. Int. J. Astrobiol. *34*, 64. https://doi.org/10.1029/2006GL027494.
14. Senatore, G., Mastroleo, F., Leys, N., and Mauriello, G. (2018). Effect of microgravity & space radiation on microbes. Future Microbiol. *13*, 831–847. https://doi.org/10.2217/fmb-2017-0251.
15. Fasnacht, M., and Polacek, N. (2021). Oxidative Stress in Bacteria and the Central Dogma of Molecular Biology. Front. Mol. Biosci. *8*, 671037. https://doi.org/10.3389/fmolb.2021.671037.
16. Milojevic, T., and Weckwerth, W. (2020). Molecular Mechanisms of Microbial Survivability in Outer Space: A Systems Biology Approach. Front. Microbiol. *11*, 923. https://doi.org/10.3389/fmicb.2020.00923.
17. Denoncin, K., and Collet, J.F. (2013). Disulfide Bond Formation in the Bacterial Periplasm: Major Achievements and Challenges Ahead. Antioxidants Redox Signal. *19*, 63–71. https://doi.org/10.1089/ars.2012.4864.
18. Seaver, L.C., and Imlay, J.A. (2001). Alkyl hydroperoxide reductase is the primary scavenger of endogenous hydrogen peroxide in Escherichia coli. J. Bacteriol. *183*, 7173–7181. https://doi.org/10.1128/Jb.183.24.7173-7181.2001.
19. Lee, J.Y., Lee, H.J., Seo, J., Kim, E.S., Lee, H.S., and Kim, P. (2014). Artificial oxidative stress-tolerant Corynebacterium glutamicum. Amb. Express *4*, 15. https://doi.org/10.1186/s13568-014-0015-1.
20. Brooks, B.E., and Buchanan, S.K. (2008). Signaling mechanisms for activation of extracytoplasmic function (ECF) sigma factors. Bba-Biomembranes *1778*, 1930–1945. https://doi.org/10.1016/j.bbamem.2007.06.005.
21. Boyd, E.S., and Barkay, T. (2012). The mercury resistance operon: from an origin in a geothermal environment to an efficient detoxification machine. Front. Microbiol. *3*, 349. https://doi.org/10.3389/fmicb.2012.00349.
22. Dik, D.A., Marous, D.R., Fisher, J.F., and Mobashery, S. (2017). Lytic transglycosylases: concinnity in concision of the bacterial cell wall. Crit Rev Biochem Mol *52*, 503–542. https://doi.org/10.1080/10409238.2017.1337705.
23. Park, J.T., and Strominger, J.L. (1957). Mode of action of penicillin. Science *125*, 99–101. https://doi.org/10.1126/science.125.3238.99.
24. Trampuz, A., Piper, K.E., Steckelberg, J.M., and Patel, R. (2006). Effect of gamma irradiation on viability and DNA of Staphylococcus epidermidis and Escherichia coli. J. Med. Microbiol. *55*, 1271–1275. https://doi.org/10.1099/jmm.0.46488-0.
25. Moreira, R.G., Puerta-Gomez, A.F., Kim, J., and Castell-Perez, M.E. (2012). Factors Affecting Radiation D-Values (D10) of an Escherichia Coli Cocktail and Salmonella Typhimurium LT2 Inoculated in Fresh Produce. J. Food Sci. *77*, E104–E111. https://doi.org/10.1111/j.1750-3841.2011.02603.x.
26. Daly, M.J., Gaidamakova, E.K., Matrosova, V.Y., Vasilenko, A., Zhai, M., Venkateswaran, A., Hess, M., Omelchenko, M.V., Kostandarithes, H.M., Makarova, K.S., et al. (2004). Accumulation of Mn(II) in Deinococcus radiodurans facilitates gamma-radiation resistance. Science *306*, 1025–1028. https://doi.org/10.1126/science.1103185.
27. Qiu, X., Daly, M.J., Vasilenko, A., Omelchenko, M.V., Gaidamakova, E.K., Wu, L., Zhou, J., Sundin, G.W., and Tiedje, J.M. (2006). Transcriptome analysis applied to survival of Shewanella oneidensis MR-1 exposed to ionizing radiation. J. Bacteriol. *188*, 1199–1204. https://doi.org/10.1128/Jb.188.3.1199-1204.2006.
28. Tapias, A., Leplat, C., and Confalonieri, F. (2009). Recovery of ionizing-radiation damage after high doses of gamma ray in the hyperthermophilic archaeon Thermococcus gammatolerans. Extremophiles *13*, 333–343. https://doi.org/10.1007/s00792-008-0221-3.
29. Margaryan, A., Badalyan, H., and Trchounian, A. (2016). Comparative Analysis of UV Irradiation Effects on Escherichia coli and Pseudomonas aeruginosa Bacterial Cells Utilizing Biological and Computational Approaches. Cell Biochem. Biophys. *74*, 381–389. https://doi.org/10.1007/s12013-016-0748-3.
30. Mackey, B.M., and Derrick, C.M. (1982). The Effect of Sublethal Injury by Heating, Freezing, Drying and Gamma-Radiation on the Duration of the Lag Phase of Salmonella-Typhimurium. J. Appl. Bacteriol. *53*, 243–251. https://doi.org/10.1111/j.1365-2672.1982.tb04683.x.
31. Bertrand, R.L. (2019). Lag Phase Is a Dynamic, Organized, Adaptive, and Evolvable Period That Prepares Bacteria for Cell Division. J. Bacteriol. *201*, e00697-18. https://doi.org/10.1128/JB.00697-18.
32. Jason, J., Cantera, L., and Stein, L.Y. (2007). Role of nitrite reductase in the ammonia-oxidizing pathway of Nitrosomonas europaea. Arch. Microbiol. *188*, 349–354. https://doi.org/10.1007/s00203-007-0255-4.
33. Brown, G.C., and Borutaite, V. (2006). Interactions between nitric oxide, oxygen, reactive oxygen species and reactive nitrogen species. Biochem. Soc. Trans. *34*, 953–956. https://doi.org/10.1042/Bst0340953.
34. Shimizu, T., Matsumoto, A., and Noda, M. (2019). Cooperative Roles of Nitric Oxide-Metabolizing Enzymes To Counteract Nitrosative Stress in Enterohemorrhagic. Infect. Immun. *87*, e00334-19. https://doi.org/10.1128/IAI.00334-19.
35. Wang, G., Alamuri, P., and Maier, R.J. (2006). The diverse antioxidant systems of Helicobacter pylori. Mol. Microbiol. *61*, 847–860. https://doi.org/10.1111/j.1365-2958.2006.05302.x.
36. Jaworek, M.W., Möbitz, S., Gao, M., and Winter, R. (2020). Stability of the chaperonin system GroEL-GroES under extreme environmental conditions. Phys. Chem. Chem. Phys. *22*, 3734–3743. https://doi.org/10.1039/c9cp06468k.
37. Hall, R.S., Fedorov, A.A., Marti-Arbona, R., Fedorov, E.V., Kolb, P., Sauder, J.M., Burley, S.K., Shoichet, B.K., Almo, S.C., and Raushel,

F.M. (2010). The Hunt for 8-Oxoguanine Deaminase. J. Am. Chem. Soc. *132*, 1762–1763. https://doi.org/10.1021/ja909817d.

38. Ragone, S., Maman, J.D., Furnham, N., and Pellegrini, L. (2008). Structural basis for inhibition of homologous recombination by the RecX protein. EMBO J. *27*, 2259–2269. https://doi.org/10.1038/emboj.2008.145.
39. Wintenberg, M., Manglass, L., Martinez, N.E., and Blenner, M. (2023). Global Transcriptional Response of Escherichia coli Exposed In Situ to Different Low-Dose Ionizing Radiation Sources. mSystems *8*, e0071822. https://doi.org/10.1128/msystems.00718-22.
40. Touati, D. (2000). Iron and oxidative stress in bacteria. Arch. Biochem. Biophys. *373*, 1–6. https://doi.org/10.1006/abbi.1999.1518.
41. Mastroleo, F., Van Houdt, R., Leroy, B., Benotmane, M.A., Janssen, A., Mergeay, M., Vanhavere, F., Hendrickx, L., Wattiez, R., and Leys, N. (2009). Experimental design and environmental parameters affect Rhodospirillum rubrum S1H response to space flight. ISME J. *3*, 1402–1419. https://doi.org/10.1038/ismej.2009.74.
42. Vajrala, N., Sayavedra-Soto, L.A., Bottomley, P.J., and Arp, D.J. (2012). Global analysis of the Nitrosomonas europaea iron starvation stimulon. Arch. Microbiol. *194*, 305–313. https://doi.org/10.1007/s00203-011-0778-6.
43. Vajrala, N., Sayavedra-Soto, L.A., Bottomley, P.J., and Arp, D.J. (2011). Role of a Fur homolog in iron metabolism in Nitrosomonas europaea. BMC Microbiol. *11*, 37. https://doi.org/10.1186/1471-2180-11-37.
44. Park, S., and Ely, R.L. (2008). Candidate stress genes of Nitrosomonas europaea for monitoring inhibition of nitrification by heavy metals. Appl. Environ. Microbiol. *74*, 5475–5482. https://doi.org/10.1128/Aem.00500-08.
45. Park, S., and Ely, R.L. (2008). Genome-wide transcriptional responses of Nitrosomonas europaea to zinc. Arch. Microbiol. *189*, 541–548. https://doi.org/10.1007/s00203-007-0341-7.
46. Chain, P., Lamerdin, J., Larimer, F., Regala, W., Lao, V., Land, M., Hauser, L., Hooper, A., Klotz, M., Norton, J., et al. (2003). Complete genome sequence of the ammonia-oxidizing bacterium and obligate chemolithoautotroph Nitrosomonas europaea. J. Bacteriol. *185*, 2759–2773. https://doi.org/10.1128/Jb.185.21.6496.2003.
47. Wei, X., Vajrala, N., Hauser, L., Sayavedra-Soto, L.A., and Arp, D.J. (2006). Iron nutrition and physiological responses to iron stress in Nitrosomonas europaea. Arch. Microbiol. *186*, 107–118. https://doi.org/10.1007/s00203-006-0126-4.
48. Blahut, M., Sanchez, E., Fisher, C.E., and Outten, F.W. (2020). Fe-S cluster biogenesis by the bacterial Suf pathway. Bba-Mol Cell Res *1867*, 118829. https://doi.org/10.1016/j.bbamcr.2020.118829.
49. Yuda, E., Tanaka, N., Fujishiro, T., Yokoyama, N., Hirabayashi, K., Fukuyama, K., Wada, K., and Takahashi, Y. (2017). Mapping the key residues of SufB and SufD essential for biosynthesis of iron-sulfur clusters. Sci. Rep. *7*, 9387. https://doi.org/10.1038/s41598-017-09846-2.
50. Frawley, E.R., and Fang, F.C. (2014). The ins and outs of bacterial iron metabolism. Mol. Microbiol. *93*, 609–616. https://doi.org/10.1111/mmi.12709.
51. Ha, S., Shin, B., and Park, W. (2018). Lack of glyoxylate shunt dysregulates iron homeostasis in Pseudomonas aeruginosa. Microbiol-Sgm *164*, 587–599. https://doi.org/10.1099/mic.0.000623.
52. Ahn, S., Jung, J., Jang, I.A., Madsen, E.L., and Park, W. (2016). Role of Glyoxylate Shunt in Oxidative Stress Response. J. Biol. Chem. *291*, 11928–11938. https://doi.org/10.1074/jbc.M115.708149.
53. Li, H., Zhou, X., Huang, Y., Liao, B., Cheng, L., and Ren, B. (2020). Reactive Oxygen Species in Pathogen Clearance: The Killing Mechanisms, the Adaption Response, and the Side Effects. Front. Microbiol. *11*, 622534. https://doi.org/10.3389/fmicb.2020.622534.
54. Charoenwong, D., Andrews, S., and Mackey, B. (2011). Role of rpoS in the Development of Cell Envelope Resilience and Pressure Resistance in Stationary-Phase Escherichia coli. Appl. Environ. Microbiol. *77*, 5220–5229. https://doi.org/10.1128/Aem.00648-11.
55. Guo, Y., Li, Y., Zhan, W., Wood, T.K., and Wang, X. (2019). Resistance to oxidative stress by inner membrane protein ElaB is regulated by OxyR and RpoS. Microb. Biotechnol. *12*, 392–404. https://doi.org/10.1111/1751-7915.13369.
56. Huang, H.H., Lin, Y.T., Chen, W.C., Huang, Y.W., Chen, S.J., and Yang, T.C. (2015). Expression and Functions of CreD, an Inner Membrane Protein in Stenotrophomonas maltophilia. PLoS One *10*, e0145009. https://doi.org/10.1371/journal.pone.0145009.
57. McCully, A.L., Behringer, M.G., Gliessman, J.R., Pilipenko, E.V., Mazny, J.L., Lynch, M., Drummond, D.A., and McKinlay, J.B. (2018). An Escherichia coli Nitrogen Starvation Response Is Important for Mutualistic Coexistence with. Appl. Environ. Microbiol. *84*, e00404-18. https://doi.org/10.1128/AEM.00404-18.
58. Cheng, Y., Yam, J.K.H., Cai, Z., Ding, Y., Zhang, L.H., Deng, Y., and Yang, L. (2019). Population dynamics and transcriptomic responses of Pseudomonas aeruginosa in a complex laboratory microbial community. Npj Biofilms Microbi *5*, 1. https://doi.org/10.1038/s41522-018-0076-z.
59. Faulkner, M.J., and Helmann, J.D. (2011). Peroxide Stress Elicits Adaptive Changes in Bacterial Metal Ion Homeostasis. Antioxidants Redox Signal. *15*, 175–189. https://doi.org/10.1089/ars.2010.3682.
60. Zwietering, M.H., Jongenburger, I., Rombouts, F.M., and Vantriet, K. (1990). Modeling of the Bacterial-Growth Curve. Appl. Environ. Microbiol. *56*, 1875–1881. https://doi.org/10.1128/aem.56.6.1875-1881.1990.
61. Ilgrande, C., Mastroleo, F., Christiaens, M.E.R., Lindeboom, R.E.F., Prat, D., Van Hoey, O., Ambrozova, I., Coninx, I., Heylen, W., Pommerening-Roser, A., et al. (2019). Reactivation of Microbial Strains and Synthetic Communities After a Spaceflight to the International Space Station: Corroborating the Feasibility of Essential Conversions in the MELiSSA Loop. Astrobiology *19*, 1167–1176. https://doi.org/10.1089/ast.2018.1973.
62. Bucur, B., Icardo, M.C., and Calatayud, J.M. (2006). Spectrophotometric determination of ammonium by an rFIA assembly. Rev. Roum. Chem. *51*, 101–108.
63. Montgomerey, H., and Dymock, J.F. (1961). Determination of Nitrite in Water, *86* (Royal Society of Chemistry Thomas Graham House), p. 414.
64. Smith, M.B., Akatov, Y., Andrews, H.R., Arkhangelsky, V., Chernykh, I.V., Ing, H., Khoshooniy, N., Lewis, B.J., Machrafi, R., Nikolaev, I., et al. (2013). Measurements of the neutron dose and energy spectrum on the International Space Station during expeditions ISS-16 to ISS-21. Radiat. Protect. Dosim. *153*, 509–533. https://doi.org/10.1093/rpd/ncs129.
65. Livak, K.J., and Schmittgen, T.D. (2001). Analysis of relative gene expression data using real-time quantitative PCR and the 2(T)(-Delta Delta C) method. Methods *25*, 402–408. https://doi.org/10.1006/meth.2001.1262.
66. Pérez, J., Buchanan, A., Mellbye, B., Ferrell, R., Chang, J.H., Chaplen, F., Bottomley, P.J., Arp, D.J., and Sayavedra-Soto, L.A. (2015). Interactions of Nitrosomonas europaea and Nitrobacter winogradskyi grown in co-culture. Arch. Microbiol. *197*, 79–89. https://doi.org/10.1007/s00203-014-1056-1.
67. Verbeelen, T., Van Houdt, R., Leys, N., Ganigué, R., and Mastroleo, F. (2023). RNA extraction protocol from low-biomass bacterial Nitrosomonas europaea and Nitrobacter winogradskyi cultures for whole transcriptome studies. STAR Protoc. *4*, 102358. https://doi.org/10.1016/j.xpro.2023.102358.
68. Liao, Y., Smyth, G.K., and Shi, W. (2013). The Subread aligner: fast, accurate and scalable read mapping by seed-and-vote. Nucleic Acids Res. *41*, e108. https://doi.org/10.1093/nar/gkt214.
69. Liao, Y., Smyth, G.K., and Shi, W. (2014). featureCounts: an efficient general purpose program for assigning sequence reads to genomic features. Bioinformatics *30*, 923–930. https://doi.org/10.1093/bioinformatics/btt656.
70. Vallenet, D., Labarre, L., Rouy, Z., Barbe, V., Bocs, S., Cruveiller, S., Lajus, A., Pascal, G., Scarpelli, C., and Médigue, C. (2006). MaGe: a microbial genome annotation system supported by synteny results. Nucleic Acids Res. *34*, 53–65. https://doi.org/10.1093/nar/gkj406.
71. Robinson, M.D., McCarthy, D.J., and Smyth, G.K. (2010). edgeR: a Bioconductor package for differential expression analysis of digital gene expression data. Bioinformatics *26*, 139–140. https://doi.org/10.1093/bioinformatics/btp616.
72. Ritchie, M.E., Phipson, B., Wu, D., Hu, Y., Law, C.W., Shi, W., and Smyth, G.K. (2015). limma powers differential expression analyses for RNA-sequencing and microarray studies. Nucleic Acids Res. *43*, e47. https://doi.org/10.1093/nar/gkv007.
73. Mastroleo, F., Arnau, C., Verbeelen, T., Mysara, M., Gòdia, F., Leys, N., and Van Houdt, R. (2022). Metaproteomics, Heterotrophic Growth, and Distribution of *Nitrosomonas europaea* and *Nitrobacter winogradskyi* after Long-Term Operation of an Autotrophic Nitrifying Biofilm Reactor. Appl. Microbiol. *2*, 272–287. https://doi.org/10.3390/applmicrobiol2010020.

STAR★METHODS

KEY RESOURCES TABLE

REAGENT or RESOURCE	SOURCE	IDENTIFIER
Bacterial and virus strains		
Nitrosomonas europaea ATCC19718	American Type Culture Collection (ATCC)	NCBI: txid228410
Nitrobacter winogradskyi Nb-255	American Type Culture Collection (ATCC)	NCBI: txid323098
Comamonas testosteroni I2	Center for Microbial Ecology and Technology (CMET), University of Ghent	NCBI: txid1440775
Chemicals, peptides, and recombinant proteins		
Lysozyme from chicken egg-white	MedChemExpress	Cat#HY-B2237
Ethylene diamine tetraacetic acid (EDTA) tetrasodium dihydrate	Sigma-Aldrich	Cat#E6511
Trizma hydrochloride (Tris-HCl)	Sigma-Aldrich	Cat#T3253
KH_2PO_4	Sigma-Aldrich	Cat#104873
K_2HPO_4	Sigma-Aldrich	Cat#60353
$NaHCO_3$	Sigma-Aldrich	Cat#S6297
NaOH	Sigma Aldrich	Cat#106498
NaClO	VWR International	Cat#27900.296
Salicyl acid	Sigma-Aldrich	Cat#84210
Sodiumnitroprusside dihydrate	VWR International	Cat#27966.180
$KHSO_4$	VWR International	Cat#27011.294
Sulfanilic acid	VWR International	Cat#20674.231
N(1-naphtyl)ethylenediamine dihydrochloride	VWR International	Cat#25792.130
Critical commercial assays		
Intracellular ATP Kit HS	BioThema AB	Cat#266-111
NucleoSpin RNA XS	Machery-Nagel	Cat#740902.50
Agilent RNA 6000 Nano Kit	Agilent Technologies	Cat#5067-1511
Illumina Ribo-Zero Plus rRNA Depletion Kit	Illumina	Cat#20037135
Illumina TruSeq Stranded Total RNA	Illumina	Cat#20020597
QiAMP DNA Mini kit	Qiagen	Cat#51304
QuantiNova SYBR Green RT-PCR kit	Qiagen	Cat#208154
Deposited data		
RNA-Seq data of *Comamonas testosteroni* control samples	This paper; NCBI SRA Database	NCBI SRA: SRR25866299
RNA-Seq data of *Comamonas testosteroni* exposed to ionizing radiation	This paper; NCBI SRA Database	NCBI SRA: SRR25866298
RNA-Seq data of *Nitrosomonas europaea* control samples	This paper; NCBI SRA Database	NCBI SRA: SRR21622767
RNA-Seq data of *Nitrosomonas europaea* exposed to IR	This paper; NCBI SRA Database	NCBI SRA: SRR25865683
RNA-Seq data of *Nitrobacter winogradskyi* control samples	This paper; NCBI SRA Database	NCBI SRA: SRR21622768
RNA-Seq data of *Nitrobacter winogradskyi* exposed to ionizing radiation	This paper; NCBI SRA Database	NCBI SRA: SRR25865679

(*Continued on next page*)

Continued

REAGENT or RESOURCE	SOURCE	IDENTIFIER
RNA-Seq data of tripartite culture control samples	This paper; NCBI SRA Database	NCBI SRA: SRR25891984
RNA-Seq data of tripartite culture samples exposed to ionizing radiation	This paper; NCBI SRA Database	NCBI SRA: SRR25891983
Oligonucleotides		
910 FW: AGCGGTGGATGATGTGGATTAA	Mastroleo et al.[73]	N/A
1141 RV: TTGTCACCGGCAGTCTCTCTAG	Mastroleo et al.[73]	N/A
urea FW: AGCGCCTTTGTGATGGAA	This paper	N/A
urea RV: GATCTGGATGTCGGGAATCATC	This paper	N/A
amoA FW: ACACCCGAGTATGTTCGTCA	Perez et al.[66]	N/A
amoA RV: TGCGATGTACGATACGACCT	Perez et al.[66]	N/A
nxrA FW: GAGATGCAGCAGACCGACTA	Perez et al.[66]	N/A
nxrA RV: GGCTGTAGACGTACCACGAA	Perez et al.[66]	N/A
Software and algorithms		
Graphpad Prism v9.5.1	GraphPad Software	https://www.graphpad.com/scientific-software/prism/
RStudio v1.4.1106	RStudio	https://www.rstudio.com/
Subread v2.0.1	Liao et al.[68]	http://subread.sourceforge.net/
edgeR v3.34.1	Robinson et al.[71]	https://bioconductor.org/packages/release/bioc/html/edgeR.html
Limma v3.48.3	Ritchie et al.[72]	https://bioconductor.org/packages/release/bioc/html/limma.html
SPSS Statistics Software v28.0.1.1	IBM Corporation	https://www.ibm.com/spss
BioAnalyzer 2100 Expert Software	Agilent Technologies	https://www.agilent.com/en/product/automated-electrophoresis/bioanalyzer-systems/bioanalyzer-software/2100-expert-software-228259
FASTQC tool v0.11.8	Brabraham Bioinformatics	https://www.bioinformatics.babraham.ac.uk/projects/fastqc/
ggplot2 v3.4.2	Hadley Wickham	https://ggplot2.tidyverse.org/
VennDiagram v1.7.3	Hanbo Chen	https://cran.r-project.org/web/packages/VennDiagram/index.html
BioRender	BioRender	www.biorender.com
Other		
BD-PND bubble detector	Bubble Technology Industries	https://bubbletech.ca/product/bd-pnd-personal-neutron-dosimeter/
BDT bubble detector	Bubble Technology Industries	https://bubbletech.ca/product/bdt-bubble-detector-thermal/

RESOURCE AVAILABILITY

Lead contact

Further information and requests for resources should be directed to and will be fulfilled by the lead contact, Felice Mastroleo (felice.mastroleo@sckcen.be).

Materials availability

This study did not generate new unique reagents.

Data and code availability

- RNA-Seq data has been deposited at the NCBI Sequence Read Archive (SRA) database and are publicly available as of the date of publication. Accession numbers are listed in the key resources table.
- This paper does not report original code.
- Any additional information required to reanalyze the data reported in this paper is available from the lead contact upon request.

EXPERIMENTAL MODEL AND SUBJECT DETAILS

Microbial strains

N. europaea ATCC 19718 was cultivated axenically in a synthetic urine salts solution (SUSS) medium based on Ilgrande et al.[3] at pH = 7.8, composed of 2.36 g/L $(NH_4)_2SO_4$, 0.15 g/L $NaNO_3$, 1.564 g/L KH_2PO_4, 2 g/L K_2HPO_4, 0.49 g/L $MgSO_4$ x $7H_2O$, 0.04 g/L $CaCl_2$ x $2H_2O$, 0.0014 g/L $FeSO_4$ x $7H_2O$, 5.2 g/L NaCl, 2.5 g/L $KHCO_3$, 3.2 g/L Na_2SO_4 x $10H_2O$ and 37.85 g/L EPPS buffer at a pH of 7.8. *N. winogradskyi* Nb-255 was grown axenically in SUSS medium where $(NH_4)_2SO_4$ was replaced by 2.46 g/L $NaNO_2$ as nitrogen source for *N. winogradskyi*, while pH was adjusted to 7.5.These cultures were subcultured by transferring 10% (v/v) of culture to fresh medium after 5–7 days of growth. *C. testosteroni* I2 was grown in SUSS medium where 0.5 g/L Na-acetate was added as a C-source and where 1.07 g/L urea was added as N-source, replacing $(NH_4)_2SO_4$. pH was adjusted to 7.0. Subcultures were made by transferring 5% (v/v) of culture to fresh SUSS medium after 2 days of growth. The tripartite culture was assembled with the separate axenic cultures of *C. testosteroni*, *N. europaea* and *N. winogradskyi*. 1/3rd of every strain was combined in a 10% (v/v) transfer to fresh SUSS medium. All cultures were incubated at 30°C in the dark on an orbital shaker shaking at 120 rpm in 250 mL red cap CELLSTAR cell culture flasks (Greiner Bio-One, Kremsmünster, Austria).

METHOD DETAILS

Determination of radiotolerance of axenic cultures

Axenic *C. testosteroni, N. europaea* and *N. winogradskyi* cultures were grown to stationary phase (2 days for *C. testosteroni,* 7 days for the nitrifiers) and exposed to a Co-60 γ-radiation source in the Lab of Nuclear Calibrations (LNK) at SCK CEN (Mol, Belgium). During irradiation, samples were shaken at 120 rpm at room temperature in the dark. All samples were exposed to a continuous dose rate of 67.29 Gy h^{-1}. Non-irradiated control samples were kept outside the irradiation bunker, in the dark and shaking at 120 rpm, at the same temperature over the same period of time. Control samples and irradiated samples were removed from the experimental setup after the latter received a predefined D_T of respectively 10 Gy, 20 Gy, 50 Gy, 100 Gy, 200 Gy, 400 Gy, 800 Gy, 1,400 Gy or 3,000 Gy. D_T was determined with calibration based on ISO 4037:2019 under the ISO 17025:2017 accreditation of the LNK facility. Four biological replicates were exposed per radiation dose.

OD_{600} measurements

The optical density was measured on 500 µL aliquots with a NanoColor UV/Vis II spectrophotometer (Machery-Nagel, Allentown, PA, USA) at wavelength λ = 600 nm (OD_{600}).

Analysis of growth after acute irradiation

After acute γ-irradiation, axenic *C. testosteroni* and nitrifier cultures were inoculated respectively 5% or 10% (v/v) in 9 mL fresh SUSS medium. OD_{600} measurements were done twice or thrice per day for *C. testosteroni* and once per day for the nitrifying cultures until stationary phase was reached or the medium was depleted. Growth curves were fitted to the Gompertz equation with unknown variables a, b and c and with y = measured OD_{600} and x = time:

$$y = a \times \exp\left[-\exp(b - cx)\right]$$

Determination of the unknown variables was performed using non-linear regression with SPSS Statistics software (version 28.0.1.1, IBM Corporation, Armonk, NY, USA). The modelled variables were transformed to biologically relevant growth kinetic parameters maximal specific growth rate (μ_{max}), lag phase (λ) and generation time (T) according to Zwietering et al..[60] Sampling and monitoring the cultures was terminated 300 h after inoculation or when the cultures were depleted.

Colony-forming unit (CFU) determination

Viability of *C. testosteroni* after exposure to acute γ-radiation was determined with CFU counting. Directly after irradiation, serial dilutions in 1x PBS were performed. 6 drops of 5 µL of culture were spotted on LB agar plates in technical duplicates. The LB agar plates were allowed to dry and incubated at 30°C overnight in the dark before counting the colonies.

Intracellular ATP measurement

Intracellular ATP to determine the amount of EAC per mL was measured in 50 µL aliquots from irradiated cultures using the Intracellular ATP Kit HS (BioThema AB, Handen, Sweden) following the manufacturer's instructions. If we consider that ATP is only present in live cells, one can calculate the amount of EAC, assuming 2×10^{-18} mol ATP equals 1 EAC as per the manufacturer's user manual.

Activity testing

Nitratation and nitritation were assessed as described in Ilgrande et al.[61] in a medium with 0.011 g/L KH_2PO_4, 0.014 g/L K_2HPO_4, 0.0025 g/L $NaHCO_3$ buffered at a pH of 7 and containing 80 mg-N/L of NH_4^+ and NO_2^-, respectively. 270 μL of activity medium was inoculated with 30 μL of the irradiated or the control samples in 96-well plates covered with Parafilm (Bemis Company, Neenah, WI, USA) and incubated at 30°C, shaking at 600 rpm in the dark. Aliquots were taken daily from the nitrifiers during 7–8 days. NH_4^+ and NO_2^- concentrations were determined colorimetrically with the Berthelot reaction and the Montgomerey reaction, respectively.[62,63]

ISS-like low-dose irradiation

Inside the ISS, the average absorbed dose in water is 280 μGy d^{-1} according to the DOSIS 3D experiment that monitored radiation on board from 2009 – 2016.[7] Neutron irradiation accounts for 30% of the total dose equivalent on board the ISS.[64] The Cf-252 neutron source was selected to simulate irradiation by high-linear energy transfer (high-LET) particles, while low-LET contribution is negligible. It is the closest approximation to the ISS radiation field available in LNK at SCK CEN. For logistical reasons, an 'accelerated life testing' approach was used to simulate *ca*. 4 months (131 days) of space irradiation inside a 3-day period of irradiation on the ground.

100 mL of axenic *C. testosteroni* was inoculated 5% (v/v) on day 0 of irradiation. 100 mL of axenic *N. europaea* and *N. winogradskyi* cultures were inoculated 10% (v/v) and grown to mid-exponential phase (3 days of growth) before irradiation. 100 mL of tripartite culture was inoculated with a 10% (v/v) inoculum consisting of 1/3rd of every axenic culture as previously described. It was grown for 20 days to ensure that all constituents of the community were active before exposure to IR. Four biological replicates of the cultures were exposed to the Cf-252 neutron radiation source with an average dose rate of 5.09 × 10^{-1} mGy h^{-1} as measured by BD-PND and BDT bubble detectors (Bubble Technology Industries, Inc., Chalk River, ON, Canada) for 72 h.

During irradiation, samples were incubated at 30°C and shaken at 120 rpm in the dark. Due to spatial limitations, the total of 16 samples was placed in front of the neutron source in 2 rows of 8 samples (Figure 6). Cultures were randomly positioned in front of the radiation source, without any specific rationale guiding their placement in the front or back row. The dose rate is inversely proportionate to the square of the distance (r) from the irradiation source ($D_T = r^{-2}$). Hence, samples in the front row experienced a higher dose rate than the samples in the back row. Because of practical restrictions in LNK, it was not possible to switch the samples at exactly half (i.e., 36h) of the total irradiation time. After 30 h, the front and back row samples were switched and the cultures were irradiated for another 42 h. Therefore, the D_T for *C. testosteroni* and the tripartite culture was 35.18 mGy, representing a 126-day stay on the ISS. For the nitrifiers, the D_T was 38.17 mGy, equivalent to a duration of 136 days on the ISS.

Relative abundance of strains in the tripartite community

DNA from the tripartite culture was extracted using the QiAMP DNA Mini kit (Qiagen, Hilden, Germany) according to the manufacturer's instructions. The relative abundance of *C. testosteroni*, *N. europaea* and *N. winogradskyi* in the tripartite culture was assessed with qPCR using the $\Delta\Delta C_T$ method.[65] Universal 16S rRNA primers 910 FW and 1141 RV (AGCGGTGGATGATGTGGATTAA, TTGTCACCGGCAGTCTCTCTAG) and species-specific primers *urea* FW and *urea* RV (AGCGCCTTTGTGATGGAA, GATCTGGATGTCGGGAATCATC), *amoA* FW and *amoA* RV (ACACCCGAGTATGTTCGTCA, TGCGATGTACGATACGACCT), and *nxrA* FW and *nxrA* RV (GAGATGCAGCAGACCGACTA, GGCTGTA GACGTACCACGAA) for *C. testosteroni*, *N. europaea* and *N. winogradskyi*, respectively, were used. Primers for *ureA* were designed for this experiment while *amoA* and *nxrA* primers were used according to Perez et al..[66] qPCR cycling parameters were 5 min at 95°C followed by 35 cycles of 15 s at 95°C and 1 min at 65°C. The program was executed on real-time PCR cycler RotorGene Q (Qiagen, Hilden, Germany). 25 μL of qPCR mixture was used with QuantiNova SYBR Green RT-PCR kit (Qiagen, Hilden, Germany), 300 nM of FW and RV primer and 5 ng of template DNA. qPCR of the genomic DNA standards, non-template controls and samples were performed in triplicate. Since *N. europaea* and *N. winogradskyi* contain 2 copies of *amoA* and *nxrA* respectively, the calculated fold change (FC) ($2^{-\Delta\Delta CT}$) for these species was divided by 2.

RNA extraction

After exposure to low-dose chronic IR, 5 mL of *C. testosteroni* and the tripartite culture, and 10 mL of the nitrifier cultures was pelleted by centrifugation at 14,000 g for 5 min. RNA was isolated with an optimized protocol for low-biomass bacterial samples as previously described Verbeelen et al. (2023).[67] Pellets were treated with a 1 mg mL^{-1} lysozyme from chicken egg-white (MedChemExpress, Monmouth Junction, NJ, USA) solution in 1x TE buffer for 15 min at 37°C. The NucleoSpin XS RNA kit was used to complete the RNA extraction as per the manufacturer's instructions. In this procedure, 200 μL RA1 buffer was used instead of 100 μL RA1 specified by the manufacturer. RNA samples with a RIN-value above or equal to 8 were accepted for sequencing. Three out of four biological replicates were selected for RNA-Seq, keeping the final replicate as a backup.

RNA sequencing

The RNA-Seq procedure was outsourced to BaseClear B.V. (Leiden, The Netherlands). In short, rRNA was depleted using the Illumina Ribo-Zero Plus kit (Illumina, San Diego, CA, USA). The Illumina TruSeq Stranded Total RNA kit (Illumina, San Diego, CA, USA) was used to construct the library. Paired-end sequence reads were generated using the Illumina NovaSeq 6000 system (Illumina, San Diego, CA, USA). FASTQ read sequence files were generated using bcl2fastq version 2.20 (Illumina, San Diego, CA, USA). Initial quality assessment was based on data

passing the Illumina Chastity filtering. Subsequently, reads containing PhiX control signal were removed using an in-house filtering protocol. In addition, reads containing (partial) adapters were clipped (up to a minimum read length of 50 bp). The second quality assessment was based on the remaining reads using the FASTQC quality control tool version 0.11.8 (Brabraham Bioinformatics, Cambridge, UK).

RNA-Seq data analysis

Paired-end mRNA reads were mapped with Subread for R (version 2.0.1)[68] to the reference genome of the strain (*C. testosteroni* I2; NCBI accession number CP067086.1, *N. europaea* ATCC19718; NCBI accession number AL954747.1, *N. winogradskyi* Nb-255; NCBI accession number CP000115.1). For the tripartite community, the 3 genomes were combined to perform the mapping process. Gene expression quantification was performed with the featureCounts function[69] from the subread package with the latest genome annotations available for *C. testosteroni* I2, *N. europaea* ATCC19718 and *N. winogradskyi* Nb-255 obtained from the MaGe platform.[70] Differential gene expression (DGE) was calculated using the edgeR (version 3.34.1)[71] and limma (version 3.48.3)[72] packages. Lowly expressed genes were filtered out. Thresholds for DGE were a p value <0.05 and a $|\log_2$ fold change $(\log_2 FC)| \geq 1$ ($|FC| \geq 2$).

Data visualization

Figures 5 and 6 were created using Biorender.com. Endpoint OD_{600}-values, growth curves, growth kinetic parameters, CFUs × mL^{-1} and the *C. testosteroni* survival curve were visualized using Graphpad Prism version 9.5.1 for Windows (GraphPad Software by Dotmatics, Boston, MA, USA). In Figure 4, Cluster of Orthologous Groups (COG) bar plots were visualized with the ggplot2 package (version 3.4.2) in R and Venn diagrams were produced with the VennDiagram package (version 1.7.3) in R.

QUANTIFICATION AND STATISTICAL ANALYSIS

Shapiro-Wilk tests were used to test for normality and unpaired t-tests were performed using Graphpad Prism version 9.5.1 for Windows to compare the endpoint OD_{600} measurements, growth kinetic parameters, CFUs × mL^{-1} of *C. testosteroni* measurements of the controls vs. the irradiated samples as displayed in Figures 1, 2, and 3; p values <0.05 were considered statistically significant. Statistical details are provided in the figure legends. Error bars represent the standard deviation from the mean. Biological quadruplicates (n = 4) were used except for RNA-Seq analysis, where biological triplicates (n = 3) were used.